



**HAL**  
open science

## Exacerbation of C1q dysregulation, synaptic loss and memory deficits in tau pathology linked to neuronal adenosine A2A receptor

Kevin Carvalho, Emilie Faivre, Marie Pietrowski, Xavier Marques, Victoria Gomez-Murcia, Aude Deleau, Vincent Huin, Jan Hansen, Stanislav Kozlov, Clément Danis, et al.

### ► To cite this version:

Kevin Carvalho, Emilie Faivre, Marie Pietrowski, Xavier Marques, Victoria Gomez-Murcia, et al.. Exacerbation of C1q dysregulation, synaptic loss and memory deficits in tau pathology linked to neuronal adenosine A2A receptor. *Brain - A Journal of Neurology*, 2019, 142 (11), pp.3636-3654. 10.1093/brain/awz288 . inserm-02350065

**HAL Id: inserm-02350065**

**<https://inserm.hal.science/inserm-02350065>**

Submitted on 5 Nov 2019

**HAL** is a multi-disciplinary open access archive for the deposit and dissemination of scientific research documents, whether they are published or not. The documents may come from teaching and research institutions in France or abroad, or from public or private research centers.

L'archive ouverte pluridisciplinaire **HAL**, est destinée au dépôt et à la diffusion de documents scientifiques de niveau recherche, publiés ou non, émanant des établissements d'enseignement et de recherche français ou étrangers, des laboratoires publics ou privés.

## Exacerbation of C1q dysregulation, synaptic loss and memory deficits in tau pathology linked to neuronal adenosine A<sub>2A</sub> receptor

Kevin Carvalho,<sup>1,\*</sup> Emilie Faivre,<sup>1,\*</sup> Marie J. Pietrowski,<sup>2,#</sup> Xavier Marques,<sup>3,#</sup> Victoria Gomez-Murcia,<sup>1</sup> Aude Deleau,<sup>1</sup>  Vincent Huin,<sup>1</sup> Jan N. Hansen,<sup>2</sup> Stanislav Kozlov,<sup>2</sup> Clément Danis,<sup>1,4</sup> Mariana Temido-Ferreira,<sup>5</sup> Joana E. Coelho,<sup>5</sup> Céline Mériaux,<sup>1</sup> Sabiha Eddarkaoui,<sup>1</sup> Stéphanie Le Gras,<sup>6</sup> Mélanie Dumoulin,<sup>7</sup> Lucrezia Cellai,<sup>1</sup> NeuroCEB Brain Bank, Isabelle Landrieu,<sup>4</sup> Yijiang Chern,<sup>8</sup> Malika Hamdane,<sup>1</sup> Luc Buée,<sup>1</sup> Anne-Laurence Boutillier,<sup>9</sup> Sabine Levi,<sup>3</sup> Annett Halle,<sup>2,10</sup> Luisa V. Lopes<sup>5</sup> and  David Blum<sup>1</sup>

\*,#These authors contributed equally to this work.

See Cunha (doi:10.1093/brain/awz335) for a scientific commentary on this article.

Accumulating data support the role of tau pathology in cognitive decline in ageing and Alzheimer's disease, but underlying mechanisms remain ill-defined. Interestingly, ageing and Alzheimer's disease have been associated with an abnormal upregulation of adenosine A<sub>2A</sub> receptor (A<sub>2A</sub>R), a fine tuner of synaptic plasticity. However, the link between A<sub>2A</sub>R signalling and tau pathology has remained largely unexplored. In the present study, we report for the first time a significant upregulation of A<sub>2A</sub>R in patients suffering from frontotemporal lobar degeneration with the *MAPT* P301L mutation. To model these alterations, we induced neuronal A<sub>2A</sub>R upregulation in a tauopathy mouse model (THY-Tau22) using a new conditional strain allowing forebrain overexpression of the receptor. We found that neuronal A<sub>2A</sub>R upregulation increases tau hyperphosphorylation, potentiating the onset of tau-induced memory deficits. This detrimental effect was linked to a singular microglial signature as revealed by RNA sequencing analysis. In particular, we found that A<sub>2A</sub>R overexpression in THY-Tau22 mice led to the hippocampal upregulation of C1q complement protein—also observed in patients with frontotemporal lobar degeneration—and correlated with the loss of glutamatergic synapses, likely underlying the observed memory deficits. These data reveal a key impact of overactive neuronal A<sub>2A</sub>R in the onset of synaptic loss in tauopathies, paving the way for new therapeutic approaches.

- 1 University of Lille, Inserm, CHU Lille, UMR-S 1172 - JPArc, LabEx DISTALZ, F-59000 Lille, France
- 2 German Center for Neurodegenerative Diseases (DZNE), Bonn, Germany
- 3 Institut du Fer à Moulin, Inserm UMR-S 1270, Sorbonne Université, F-75005, Paris, France
- 4 University of Lille, CNRS UMR8576, Unité de Glycobiologie Structurale et Fonctionnelle, LabEx DISTALZ, Lille, F-59000 Lille, France
- 5 Instituto de Medicina Molecular, Faculdade de Medicina de Lisboa, Universidade de Lisboa, Lisbon, Portugal
- 6 CNRS, Inserm, UMR 7104, GenomEast Platform, Institut de Génétique et de Biologie Moléculaire et Cellulaire (IGBMC), Université de Strasbourg, F-67400 Illkirch, France
- 7 University of Lille, F-59000 Lille, France
- 8 Institute of Biomedical Sciences, Academia Sinica, Taipei, Taiwan
- 9 Laboratoire de Neurosciences Cognitives et Adaptatives (LNCA), CNRS UMR 7364, Université de Strasbourg, F-67000 Strasbourg, France
- 10 Institute of Neuropathology, University of Bonn Medical Center, Bonn, Germany

Received March 19, 2019. Revised July 24, 2019. Accepted July 26, 2019. Advance Access publication October 10, 2019

© The Author(s) (2019). Published by Oxford University Press on behalf of the Guarantors of Brain.

This is an Open Access article distributed under the terms of the Creative Commons Attribution Non-Commercial License (<http://creativecommons.org/licenses/by-nc/4.0/>), which permits non-commercial re-use, distribution, and reproduction in any medium, provided the original work is properly cited. For commercial re-use, please contact [journals.permissions@oup.com](mailto:journals.permissions@oup.com)

Correspondence to: David Blum  
Inserm UMR-S1172, 'Alzheimer & Tauopathies', Place de Verdun, 59045, Lille Cedex,  
France  
E-mail: david.blum@inserm.fr

**Keywords:** adenosine; A<sub>2A</sub> receptor; tau; microglia; C1q

**Abbreviations:** A<sub>2A</sub>R = adenosine A<sub>2A</sub> receptor; FTLD = frontotemporal lobar degeneration

## Introduction

Tau pathology is defined by the accumulation of hyperphosphorylated and aggregated tau proteins in neurofibrillary tangles (Sergeant *et al.*, 2008). During ageing, tau pathology in the temporal lobe of aged individuals has been linked to memory decline (Duyckaerts *et al.*, 2015; Josephs *et al.*, 2017). Tau pathology is also the defining neuropathological hallmark of a class of neurodegenerative diseases, called tauopathies, including Alzheimer's disease and frontotemporal lobar degeneration with tau aggregation (FTLD-tau), such as progressive supranuclear palsy (PSP), corticobasal degeneration (CBD) and Pick's disease as well as inherited diseases caused by mutation in the *MAPT* gene coding tau (Hutton *et al.*, 1998; Mackenzie and Neumann, 2016; Lebouvier *et al.*, 2017). In Alzheimer's disease, the progression of tau pathology from entorhinal cortex, hippocampus, and finally neocortex corresponds to the progression of clinical symptoms (Duyckaerts *et al.*, 1997; Grober *et al.*, 1999; Jucker and Walker, 2013), suggesting a central role in the development of cognitive deficits. However, pathways underlying tau pathology-induced cognitive deficits remain ill-defined.

Compelling evidence has implicated adenosine A<sub>2A</sub> receptor (A<sub>2A</sub>R) in age-dependent cognitive impairment (for review see Cunha, 2016). A<sub>2A</sub>R is a druggable G-protein-coupled receptor whose endogenous ligand is adenosine, an important modulator of synaptic activity, particularly in the hippocampus (Cunha, 2016). Several studies consistently described increased expression, density and function of A<sub>2A</sub>R in the hippocampus of aged animals, occurring at glutamatergic nerves terminals (Lopes *et al.*, 1999; Rebola *et al.*, 2003; Canas *et al.*, 2009a; Costenla *et al.*, 2011). Recently, we demonstrated a neuronal upsurge of A<sub>2A</sub>R in the hippocampus of aged individuals that was further enhanced in patients with Alzheimer's disease (Temido-Ferreira *et al.*, 2018). Interestingly, neuronal enhancement of A<sub>2A</sub>R signalling was shown to recapitulate an ageing-like phenotype, characterized by hypothalamic-pituitary-adrenal axis dysfunction, altered synaptic plasticity and memory deficits (Batalha *et al.*, 2013, 2016; Li *et al.*, 2015; Temido-Ferreira *et al.*, 2018).

The link between A<sub>2A</sub>R signalling and tau pathology has remained largely unexplored. A previous study reported a significant upregulation of A<sub>2A</sub>R (*ADORA2A*) mRNA and increased A<sub>2A</sub>R signalling in the frontal cortex of patients with Pick's disease, a tauopathy (Albasanz *et al.*, 2006). More recently, a study revealed a correlation between

hippocampal A<sub>2A</sub>R mRNA expression, the Braak stages and cognitive impairment in patients with Alzheimer's disease (Orr *et al.*, 2015), suggesting that tau-dependent A<sub>2A</sub>R upsurge may favour the development of cognitive deficits in tauopathies. In the present study, we demonstrate an association between neuronal upregulation of A<sub>2A</sub>R and tau pathology in the cortex of FTLD patients with the *MAPT* P301L mutation. Promoting neuronal A<sub>2A</sub>R upregulation in a tauopathy mouse model (THY-Tau22) led to a hippocampal upregulation of C1q complement protein associated with a loss of glutamatergic synapses and a potentiation of spatial memory deficits, suggesting an instrumental role of neuronal A<sub>2A</sub>R dysregulation towards tau pathology-induced cognitive alterations.

## Materials and methods

### Post-mortem brain samples

Post-mortem brain tissue was obtained from brain banks at university medical centres in Lille (France), Paris (France) and Geneva (Switzerland), following approval by the local institutional review board and the provision of written, informed consent by the donor's family. We used samples from the temporal cortex of three FTLD-tau patients with *MAPT* P301L mutation (Forrest *et al.*, 2018) and three age-matched controls (control group A) obtained from NEUROCEB brain bank. We also used samples from Brodmann area 10 in frontal brain region from 10 patients with sporadic FTLD-tau (five CBD and five Pick's disease) and nine other age-matched controls (control group B), obtained from the brain banks of Lille, Paris and Geneva. Controls were defined as individuals with no signs of cognitive decline, no history of stroke or chronic brain pathology and a Braak stage of 0 to 2. All patients and tissues have been diagnosed by trained pathologists. Diseased individuals and control subjects did not significantly differ in their mean age at death [FTLD-tau P301L patients, 58 ± 7.5 years of age; control group A, 65 ± 6 years of age;  $P = 0.5$ , Student's *t*-test; mean ± standard error of the mean (SEM); CBD patients, 75 ± 1.8 years of age; Pick's disease patients, 66.8 ± 1.8; control group B, 75 ± 3.9 years of age;  $P > 0.5$ , ANOVA; mean ± SEM). They did not differ in the mean post-mortem interval (FTLD-tau P301L, 18.0 ± 9.8 h; control group A, 22.0 ± 7.5 h;  $P = 0.78$ ; Student's *t*-test; mean ± SEM; CBD patients, 15.8 ± 5.0 h; Pick's disease patients, 15.7 ± 2.9 h; control group B, 18.3 ± 6.1 h;  $P > 0.5$ , ANOVA; mean ± SEM). Most participants and methods have been described previously (Huin *et al.*, 2016). Fresh frozen temporal grey matter tissue (~100 mg) retrieved at autopsy and stored at -80°C was used for western blot or

quantitative PCR. Formalin-fixed and paraffin-embedded temporal grey matter tissue was used for immunohistology in 8- $\mu$ m thick sections.

## Generation of A<sub>2A</sub>R inducible transgenic mice

To generate the TRE-A<sub>2A</sub>R transgenic line, an optimized cDNA sequence of the 410-amino acid murine A<sub>2A</sub>R flanked upstream by a ClaI site and a Kozak consensus sequence (GCCACC; Kozak, 1987) and downstream by a WRE sequence (the Woodchuck hepatitis virus responsive element; GenBank accession number: J04514) and EcoRV site was generated by GeneArt (named 11AASNZC-mAdora2a). This 1843-bp sequence (Supplementary Fig. 1) was inserted into a modified pTRE-Tight-BI-AcGFP1 vector (Clontech) at the ClaI-EcoRV site of the multiple cloning site; the vector modification consisted of adding HindIII site at position 2522. The transgene fragment (4617 bp) obtained after HindIII-VspI digestion includes the following sequences: SV40 polyadenylation signal, *AcGFP1* gene, the bidirectional inducible *P*<sub>tight</sub> Tet-responsive promoter, 11AASNZC-mAdora2a, SV40 polyadenylation signal. This fragment was used for standard pronuclear injections in C57BL/6N background (SEAT, UPS44, CNRS). Genotyping was performed by PCR using the following primers: forward: 5'-ACACAGGAACACCAGGAAGG-3', reverse: 5'-CAACACCACGGAATTGTCAG-3' allowing amplification of a 492-bp fragment. The selected founder line was backcrossed to C57BL/6J for more than 10 generations.

## Conditional mouse model of neuronal A<sub>2A</sub>R overexpression

All animals were maintained in groups of five to six in ventilated cages in a SOPF (specific opportunist pathogen free) facility (12-h/12-h light/dark cycle, 22°C), with *ad libitum* access to food (SafeA04) and water. The animals were maintained in compliance with European standards for the care and use of laboratory animals and experimental protocols approved by the local Animal Ethical Committee (agreement #12787-2015101320441671 v9 from CEEA75, Lille, France). The overexpression of mouse A<sub>2A</sub>R in forebrain neurons was achieved by crossing the in-house developed TRE-A<sub>2A</sub>R transgenic strain (in which mouse receptor cDNA is under the control of a Tet-responsive element) and the transgenic CaMKII-tTA line, expressing the tetracycline-controlled transactivator protein (tTA) under regulatory control of the forebrain-specific calcium-calmodulin-dependent kinase II (CaMKII) promoter [B6.Cg-Tg(Camk2a-tTA)1Mmay/DboJ; SN 7004; The Jackson Laboratory; Fig. 2A]. Previously, the tTA transactivator was found to favour hippocampal atrophy in non-C57Bl6 genetic backgrounds (Han *et al.*, 2012). According to this study, evaluation of hippocampal morphology (Cresyl violet) did not reveal morphological modifications in CaMKII-tTA transgenic mice versus littermate wild-type in both CA1 and dentate gyrus (Supplementary Fig. 2). The CaMKII promoter drives expression in forebrain neurons with low level at birth strongly increasing from postnatal Days 7 to 25 (Kelly *et al.*, 1987; Scholz *et al.*, 1988; Burgin *et al.*, 1990). As adenosine signalling may play some role during neurodevelopment (Rodrigues *et al.*, 2018), the A<sub>2A</sub>R transgene was maintained off by doxycycline oral treatment (0.2 mg/ml in 2.5% sucrose

in drinking water) from mating to offspring weaning. Tetracyclines have been shown to provide anti-inflammatory effects (Blum *et al.*, 2004) and doxycycline in particular has been shown to counteract the development of neuroinflammation in an Alzheimer's disease model (Balducci *et al.*, 2018). As we intended to cross our new conditional transgenic model with tau transgenic mice (see below), which develop neuroinflammation (Laurent *et al.*, 2017), we evaluated if doxycycline treatment of dams from mating to weaning would eventually interfere with the later development of induced-neuroinflammation in the adult progeny. To this aim, we analysed the hippocampal response 24 h after intraperitoneal lipopolysaccharide (LPS, L4391 Sigma) injection (0.1 or 5 mg/kg, diluted in PBS) of adult C57Bl6/J (2-month-old) mice originating from doxycycline or vehicle-treated dams. While expression of several inflammatory markers (such as IL1B, TNFA and CCL3) was found significantly increased in the hippocampus 24 h following LPS injection, doxycycline treatment of dams did not modulate the development of LPS-induced neuroinflammation in adults (Supplementary Fig. 3).

## Generation of a new transgenic model of forebrain A<sub>2A</sub>R overexpression in a THY-Tau22 background

THY-Tau22 mice (C57BL6/J background; Schindowski *et al.*, 2006) were crossed with TRE-A<sub>2A</sub>R mice to generate THY-Tau22/TRE-A<sub>2A</sub>R male mice. The latter were crossed with CaMKII-tTA females. Eight genotypic heterozygous groups were obtained: wild-type, CaMKII-tTA, TRE-A<sub>2A</sub>R, CaMKII-tTA/TRE-A<sub>2A</sub>R, THY-Tau22, THY-Tau22/CaMKII-tTA, THY-Tau22/TRE-A<sub>2A</sub>R and THY-Tau22/CaMKII-tTA/TRE-A<sub>2A</sub>R. Wild-type and THY-Tau22 mice were not used. Spontaneous activity (Supplementary Fig. 4A and B), anxiety-like behaviour (Supplementary Fig. 4C) and spatial memory (Supplementary Fig. 4D) of CaMKII-tTA versus TRE-A<sub>2A</sub>R (Supplementary Fig. 4A–D) and THY-Tau22/CaMKII-tTA versus THY-Tau22/TRE-A<sub>2A</sub>R groups were similar. Further, tau hyperphosphorylation did not differ between THY-Tau22/CaMKII-tTA and THY-Tau22/TRE-A<sub>2A</sub>R animals (Supplementary Fig. 4E). Therefore, for subsequent analysis CaMKII-tTA and TRE-A<sub>2A</sub>R were pooled as a single group ('wild-type' or 'WT') as well as THY-Tau22/CaMKII-tTA and THY-Tau22/TRE-A<sub>2A</sub>R ('tau'). The CaMKII-tTA/TRE-A<sub>2A</sub>R (double transgenic mice overexpressing neuronal A<sub>2A</sub>R) and THY-Tau22/CaMKII-tTA/TRE-A<sub>2A</sub>R (triple transgenic mice overexpressing neuronal A<sub>2A</sub>R in tau context) were identified as 'A<sub>2A</sub>R' and 'tau/A<sub>2A</sub>R', respectively. In addition, both males and females were used for behavioural characterization and pooled for analysis, as no major sex differences were found in THY-Tau22 mice (Laurent *et al.*, 2016; not shown).

## Behavioural studies

Behavioural experiments were conducted with animals between 5 to 6 months of age, randomly assigned, by experimenters blinded to the genotype of mice. Procedures are given in the Supplementary material.

## Preparation of mouse brain

Animals were euthanized (morning time) at 6 months of age. Males were sacrificed by cervical dislocation, brains were harvested, left and right hippocampi were dissected out using a coronal acrylic slicer (Delta Microscopies) at 4°C and stored at –80°C for biochemical and mRNA analyses. Females, used for immunohistochemical studies, were deeply anaesthetized with pentobarbital sodium (50 mg/kg, intraperitoneally), then transcardially perfused with cold NaCl (0.9%) and with 4% paraformaldehyde in PBS (pH 7.4). Brains were removed, post-fixed for 24 h in 4% paraformaldehyde and cryoprotected in 30% sucrose before being frozen at –40°C in isopentane (methyl-butane) and stored at –80°C. Coronal brain sections (35 µm) were obtained using a Leica cryostat. Free-floating sections were chosen according to the stereological rules, with the first section taken at random and every 12 sections afterwards, and were stored in PBS-azide (0.2%) at 4°C.

## Immunostaining

Procedures for human and mouse tissue immunostaining are supplied in the Supplementary material.

## Analysis of immunostainings

### Analysis of A<sub>2A</sub>R immunostaining in human tissue

Quantification of A<sub>2A</sub>R staining intensity within AT8-positive versus AT8-negative cells on sections from FTLT-tau patients and age-matched controls was performed using the Imaris Cell module (Bitplane, USA). Analysis was performed in 9 to 11 3D-reconstructed images per individual, representing 30 images per condition.

### Quantitative VGAT and VGLUT1 analysis

We determined regions of interest in the molecular layer and in the hilus. Quantification of VGAT and VGLUT1 was performed using MetaMorph software (Roper Scientific). Images were first flattened background filtered (kernel size, 3 × 3 × 2) to enhance cluster outlines, and an intensity threshold was applied automatically and confirmed visually to select appropriate clusters and avoid their coalescence. The total number of VGAT or VGLUT1 clusters in each region of interest (total number per 581 µm<sup>2</sup>) was quantified.

### Analysis of microglia

Cell number and morphology of Iba1-immunolabeled microglia were quantified in 12 and eight confocal images of the CA1 and dentate gyrus regions, respectively, per animal using custom-written ImageJ plugins. For quantification of cell number, confocal images were pre-processed by enhancing contrast (settings: 0.4% saturated, normalized) and generating substacks of eight z-slices. Substacks were processed by the following ImageJ functions to obtain a binary image: (i) Subtract Background (settings: rolling, 50 px corresponding to 7.44 µm); (ii) Enhance Contrast (0.4% saturated, normalize); (iii) Convert to 8-bit; (iv) Auto Local Threshold (method Bernsen, radius = 15 px corresponding to 2.23 µm, parameter1 = 0, parameter2 = 0, white objects on black background); and (v) Fill Holes. A new empty image of the same size was generated and a 3D ellipsoid was fitted to the binary

image (radius *x* and *y*: 1.2 µm; radius *z*: 1.0 µm) at each pixel position. If all pixels in a fitted ellipsoid were positive in the binary image, all corresponding pixels in the new image were set to the maximum intensity value. Each 3D particle in the new image was defined as a microglia soma. The soma number, i.e. the number of 3D particles in the new image, was quantified. Automatic soma detection was scrutinized by a trained and blinded observer and corrected manually, if required. 3D analysis of microglial morphology was performed with custom-written ImageJ plugins similar to what has been described (Plescher *et al.*, 2018). Briefly, confocal images were substacked and preprocessed using contrast enhancement of 0.1% and Gaussian blur filter (sigma 2.0). Segmented binary images were generated automatically. To this end, an intensity threshold was calculated individually for each image in an 8-bit converted, 0.5-fold scaled maximum intensity projection using the ‘Li’ algorithm and applied to the preprocessed image stack. Binary images were subsequently filtered using a 3D particle filter, maintaining particles above 13 000 voxels corresponding to 231.45 µm<sup>3</sup>. The morphology of the remaining 3D objects, i.e. individual microglial cells and their cell skeleton was analysed subsequently, deriving the following morphological parameters: ramification index (ratio of cell surface and cell volume), total dendritic tree length (total length of all cell branches), and spanned volume (convex hull volume of a cell). A Gaussian filter (sigma 1.0) was applied prior to skeletonization. Segmented 3D objects above a volume of 1400 µm<sup>3</sup> represented doublets or triplets of individual microglia and were excluded from analysis. To exclude cells close to the border of an image, only cells with their soma 20 µm distant from the border in *x* and *y* directions and between 4 µm and 6 µm in depth of the stack (*z*-direction) were included in the analysis, resulting in ~250 and ~150 analysed microglial cells per animal in the CA1 and dentate gyrus regions, respectively.

## Biochemistry

Biochemical procedures for human and mouse tissue are provided in the Supplementary material.

## RNA extraction and quantitative real-time reverse transcription polymerase chain reaction

RNA extraction and quantitative real-time reverse transcription polymerase chain reaction were performed as described previously (Laurent *et al.*, 2016, 2017). Sequences of primers used in this study are given in Supplementary Table 2. Cyclophilin A was used as a reference housekeeping gene for normalization.

### RNA sequencing

RNA-seq libraries (*n* = 4/group) were generated from 300 ng of total RNA using Illumina TruSeq RNA Sample Preparation Kit v2 (Illumina RS-122-2101). Briefly, following purification with poly-T oligo attached magnetic beads, the mRNA was fragmented using divalent cations at 94°C for 2 min. The cleaved RNA fragments were copied into first-strand cDNA using reverse transcriptase and random primers. Second-strand cDNA was synthesized using DNA polymerase I and RNase H. Following

the addition of a single ‘A’ base and subsequent ligation of the adapter on double-stranded cDNA fragments, the products were purified and enriched with PCR [30 s at 98°C; (10 s at 98°C, 30 s at 60°C, 30 s at 72°C) × 12 cycles; 5 min at 72°C] to create the cDNA library. Surplus PCR primers were removed by purification using AMPure XP beads (Beckman Coulter), and the final cDNA libraries were checked for quality and quantified using capillary electrophoresis. Sequencing was performed on the Illumina Genome HiSeq 4000 as single-end 50-base reads following manufacturer’s instructions. Reads were mapped onto the mm10 assembly of mouse genome using tophat-2.0.14 (Trapnell *et al.*, 2009) and the bowtie version: bowtie-2-2.1.0 (Langmead *et al.*, 2009). Only uniquely aligned reads were retained for further analyses. Quantification of gene expression was performed using HTSeq-0.6.1 (Anders *et al.*, 2015) and gene annotations from Ensembl release 90. Read counts were normalized across libraries with the method proposed by Anders and Huber (2010). Differential expression analysis was conducted using the method proposed by Love *et al.* (2014) implemented in the DESeq2 Bioconductor library (DESeq2 v1.14.1). *P*-values were adjusted for multiple testing using the Benjamini and Hochberg method (Benjamini and Hochberg, 1995). Gene ontology (GO) analyses for functional enrichments were performed using the tools DAVID (Huang *et al.*, 2009) and/or STRING (©STRING Consortium 2018; Szklarczyk *et al.*, 2017). Whole mouse genome (mm10) was used as background. Top-enriched terms are shown (*P*-values < 0.05 were considered).

## Electrophysiological recordings

Animals were euthanized by cervical dislocation, decapitated, the brain rapidly removed and the hippocampi dissected in ice-cold Krebs solution composed of (mM): NaCl 124; KCl 3; NaH<sub>2</sub>PO<sub>4</sub> 1.25; NaHCO<sub>3</sub> 26; MgSO<sub>4</sub> 1; CaCl<sub>2</sub> 2; and glucose 10 (previously gassed with 95% O<sub>2</sub> and 5% CO<sub>2</sub>, pH7.4). Slices (400-µm thick) were obtained with a McIlwain tissue chopper, left to recover for at least 1 h in Krebs solution, and field excitatory postsynaptic potentials (fEPSPs) were recorded as described previously in the CA1 stratum radiatum (Batalha *et al.*, 2013). Drug SCH 58261 (50 nM), was added to the Krebs superfusion solution (3 ml/min) after obtaining a stable baseline for 30 min.

## Statistics

Image acquisition and quantification as well as behavioural evaluations were performed by investigators blind to the experimental condition. Results are expressed as means ± standard error of the mean (SEM). Differences between mean values were determined using the two-tailed unpaired Student’s *t*-test, two-way ANOVA or one-way ANOVA, followed by a *post-hoc* Tukey’s multiple comparisons test using GraphPad Prism Software. *P*-values < 0.05 were considered significant.

## Data availability

The data that support the findings of this study are available on request to the corresponding author.

## Results

### A<sub>2A</sub>R upregulation in the temporal cortex of patients with FTL D carrying the MAPT P301L mutation

To establish a potential link between A<sub>2A</sub>R dysregulation and tau pathology, we evaluated levels of A<sub>2A</sub>R by western blot and immunohistochemistry on human brain samples from FTL D-tau patients carrying the MAPT P301L mutation, a pure tauopathy. Biochemical and immunohistological analyses demonstrated a significant increase of A<sub>2A</sub>R levels in the temporal cortex of FTL D-tau patients as compared to age-matched individuals [Fig. 1A and B(i)]. Interestingly, following AT8/A<sub>2A</sub>R co-immunostaining in FTL D-tau patients, we could also observe that A<sub>2A</sub>R immunoreactivity was significantly increased in neurons exhibiting tau pathology (indicated by an arrow) compared to AT8-negative cells (indicated by an asterisk) [Fig. 1B(ii)], suggesting an association between the development of tauopathy and A<sub>2A</sub>R neuronal upregulation.

### A conditional (Tet-Off) transgenic mouse model of neuronal A<sub>2A</sub>R overexpression

To delineate the impact of neuronal A<sub>2A</sub>R dysregulation on the development of tau pathology and associated cognitive deficits, we developed a transgenic mouse model allowing a conditional neuron-specific A<sub>2A</sub>R overexpression (Fig. 2A). A<sub>2A</sub>R overexpression was achieved by the crossing of a new mouse line carrying a mouse A<sub>2A</sub>R transgene under the control of a Tet-responsive element (TRE-A<sub>2A</sub>R strain) with a transgenic model expressing the tetracycline-controlled transactivator protein under the control of a neuronal forebrain CaMKII promoter (CaMKII-tTA strain; Fig. 2A). The A<sub>2A</sub>R transgene expression was maintained off from mating to offspring weaning [postnatal Day (P)28] by doxycycline treatment, to avoid any perinatal effects. As expected, endogenous A<sub>2A</sub>R was highly enriched in the striatum (Blum *et al.*, 2003), in CaMKII-tTA/TRE-A<sub>2A</sub>R mice (A<sub>2A</sub>R group) and in littermate controls (wild-type group) under doxycycline treatment (Fig. 2C, middle). In the absence of doxycycline (transgene ON) during mating (Fig. 2B and C, left) or 5 months post-doxycycline removal from P28 (Fig. 2B and C, right), a significant A<sub>2A</sub>R overexpression was found in forebrain areas of CaMKII-tTA/TRE-A<sub>2A</sub>R mice, particularly in the hippocampus and the cortex.

Co-immunostaining using antibodies raised against neuronal (NeuN), interneuron (GAD67), microglia (Iba1) and astrocytic (GFAP, S100β) markers revealed, in the hippocampus, the presence of A<sub>2A</sub>R exclusively in pyramidal and granular neurons (Figs 2D, E and 4A) but not in GABAergic interneurons (Supplementary Fig. 6) or doublecortin-positive neuronal

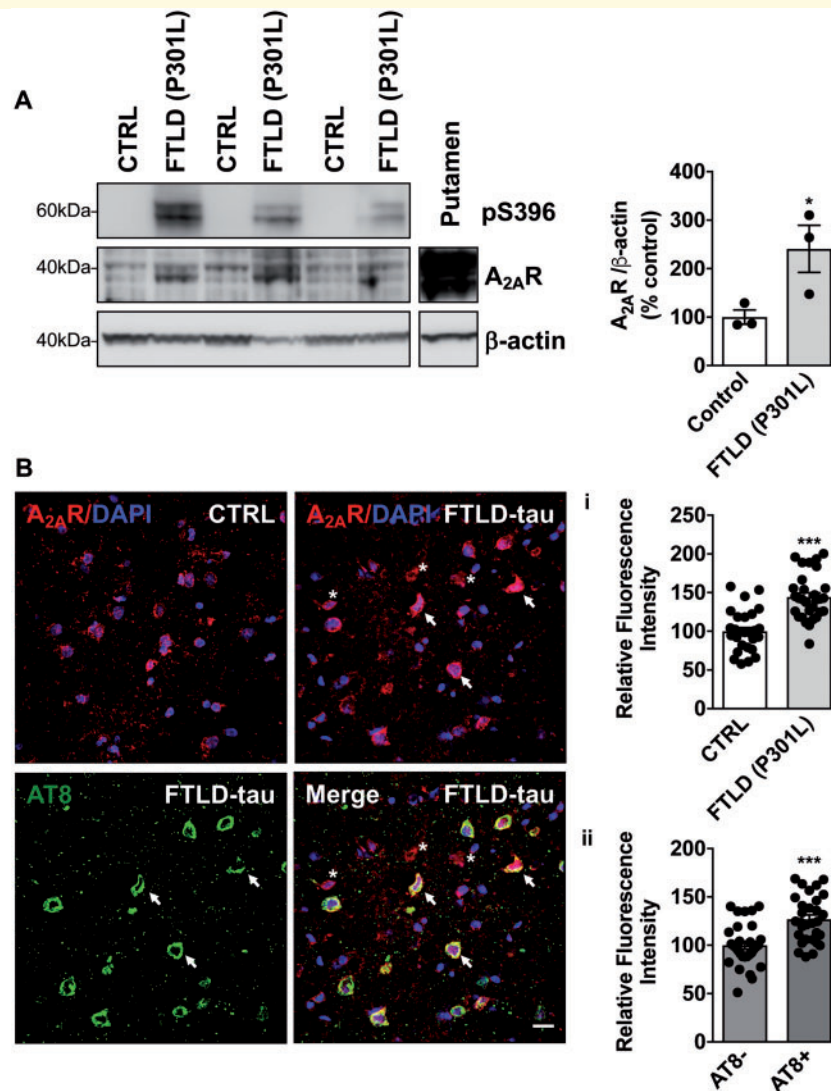


**Figure 1** A<sub>2A</sub>R upregulation in the temporal cortex of patients with frontotemporal dementia (FTLD-tau) carrying P301L mutations. **(A)** Western blot analysis of tau phosphorylation at S396 and A<sub>2A</sub>R expression in the cortex of FTLD-tau patients and age-matched controls (CTRL). Data revealed an expected tau hyperphosphorylation at S396 in the cortex of FTLD-tau patients as well as a significant increase of A<sub>2A</sub>R expression. \**P* < 0.05 versus Control using Student's *t*-test. *n* = 3 per group. Putamen sample was used as a positive control for A<sub>2A</sub>R immunoreactivity. **(B)** Immunohistochemical detection of A<sub>2A</sub>R in the temporal cortex from the same FTLD-tau patients and age-matched controls. Staining intensity was first measured in individual A<sub>2A</sub>R<sup>+</sup> cells (red) detected in controls (*n* = 1616 cells) and FTLD-tau patients (*n* = 2153 cells) from 9–11 region of interests per individual representing *n* = 29–30 images per group overall. In line with biochemical data, quantitative immunohistochemical evaluation indicated an upsurge of cellular A<sub>2A</sub>R expression in the cortex of FTLD-tau patients (i). In addition, in FTLD-tau patients, A<sub>2A</sub>R staining intensity was compared between neurons exhibiting tau pathology i.e. AT8-positive (green, indicated by an arrow; *n* = 370) and AT8-negative cells (indicated by an asterisk; *n* = 1818) from 9–11 region of interests per individual representing 30 images per group overall. Analysis revealed a higher A<sub>2A</sub>R staining intensity in AT8-positive neurons as compared to AT8-negative cells (ii). DAPI (blue) represents cell nuclei. \*\*\**P* < 0.001 versus Control using Student's *t*-test. Results are expressed as mean ± SEM. Scale bar = 20 μm.

precursor cells (Fig. 2E). To address the functionality of neuronally-overexpressed A<sub>2A</sub>R, we recorded fEPSPs from the CA1 area. As shown in Fig. 2F, A<sub>2A</sub>R blockade by the selective antagonist SCH58261, significantly inhibited fEPSPs, an effect that was not observed in wild-type animals. These data demonstrated a gain of function of A<sub>2A</sub>R that exerts a tonic control on basal synaptic transmission in CaMKII-tTA/TRE-A<sub>2A</sub>R mice.

## Neuronal overexpression of A<sub>2A</sub>R accelerates spatial memory deficits of tau transgenic mice

To assess the impact of neuronal A<sub>2A</sub>R dysregulation on the development of tau pathology and associated memory impairment, we explored the outcome of neuronal A<sub>2A</sub>R

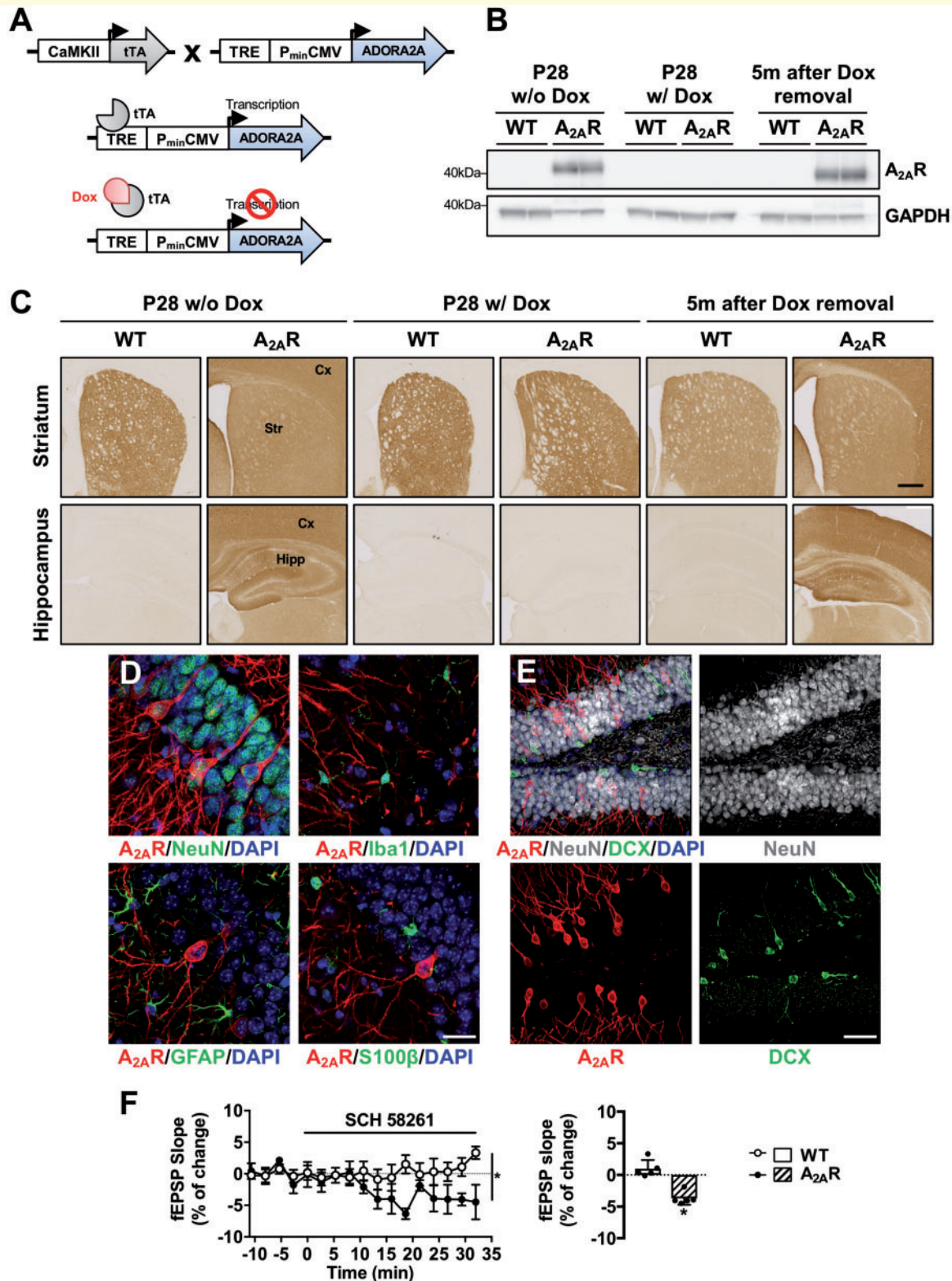


**Figure 2** Conditional (Tet-Off) transgenic mouse model of neuronal A<sub>2A</sub>R overexpression. (A) Conditional overexpression of A<sub>2A</sub>R in neurons is achieved by crossing of CaMKII-tTA mice, expressing the transactivator protein tTA, under the control of a neuronal forebrain promoter (CaMKII) with the TRE-A<sub>2A</sub>R strain, in which murine A<sub>2A</sub>R is under the control of a Tet-responsive element. A<sub>2A</sub>R expression is elicited in CaMKII-expressing neurons by the binding of the tTA protein to the TRE promoter. Transgene expression is maintained off from mating until offspring weaning (P28) by doxycycline (0.2 mg/ml in drinking water) to avoid potential perinatal effects linked to early A<sub>2A</sub>R overexpression. (B) Representative western blots of A<sub>2A</sub>R in the hippocampus of double CaMKII-tTA/TRE-A<sub>2A</sub>R (A<sub>2A</sub>R mice) and littermate controls (WT, wild-type). In absence of doxycycline, at P28 (P28 w/o Dox, left), double transgenic A<sub>2A</sub>R animals exhibited receptor immunoreactivity while its level

(continued)

overexpression in the THY-Tau22 (tau) transgenic mouse line, which progressively develops hippocampal tau pathology and spatial memory deficits (Van der Jeugd *et al.*, 2011, 2013; Burnouf *et al.*, 2013). To this end, double THY-Tau22/TRE-A<sub>2A</sub>R animals were crossed with CaMKII-tTA animals to generate THY-Tau22/TRE-A<sub>2A</sub>R/CaMKII-tTA triple transgenic mice (referred to as ‘tau/A<sub>2A</sub>R’) and littermate controls. Animals were evaluated at an early time point in pathology development i.e. at 5–6 months, when hippocampal tau pathology is developing but memory alteration remains limited (Van der Jeugd *et al.*, 2013). Using actimetry, no difference in spontaneous activity was observed with similar distance travelled (Fig. 3A) and velocity (Fig. 3B) among the different groups. Using the elevated-plus maze, as expected from previous studies (Schindowski *et al.*, 2006), we observed that tau mice spent more time in open arms as compared to littermate controls. However, A<sub>2A</sub>R neuronal overexpression did not impact anxiety-related behaviour either in control (A<sub>2A</sub>R group) or tau (tau/A<sub>2A</sub>R group) mice (Fig. 3C). Next, we evaluated spatial memory using the Barnes maze. During the learning phase, all groups showed a decrease in path length across trials ( $P < 0.001$ , Fig. 3D), indicating proper spatial learning abilities. As compared to control animals (wild-type), A<sub>2A</sub>R, tau and tau/A<sub>2A</sub>R mice demonstrated a slight learning impairment at Day 2 ( $P < 0.01$ ). Neither tau nor A<sub>2A</sub>R overexpression influenced mouse velocity (data not shown). Twenty-four hours following acquisition, a probe trial was performed to assess spatial memory. Regardless of A<sub>2A</sub>R expression, wild-type animals exhibited a significant preference for the target quadrant (Fig. 3E, wild-type:  $P < 0.001$  and A<sub>2A</sub>R-overexpressing mice:  $P < 0.05$  versus non-target quadrant) and spent a significantly greater proportion of time in the latter than expected by chance (i.e.  $>25\%$ ; wild-type:  $56.7 \pm 3.8\%$ ,  $P < 0.001$ ; A<sub>2A</sub>-overexpressing mice:  $39.9 \pm 5.4\%$ ,  $P < 0.001$ ; one sample *t*-test). However, in line with our previous studies (Batalha *et al.*, 2016; Temido-Ferreira *et al.*, 2018), neuronal overexpression of A<sub>2A</sub>R reduced memory performance with A<sub>2A</sub>R animals spending less time in the target quadrant as compared

to wild-type ( $P < 0.05$  versus wild-type), although their preference for the target quadrant remained significant. As expected at this age (Van der Jeugd *et al.*, 2013), tau mice did not exhibit spatial memory impairment, evidenced by a significant preference for the target over the non-target quadrants ( $P < 0.001$ ), a significantly greater proportion of time spent in the former than expected by chance ( $50.8 \pm 4.3\%$ ,  $P < 0.001$ ) and a similar percentage of time spent in the target quadrant compared to wild-type animals ( $P = 0.85$ ). In sharp contrast, neuronal A<sub>2A</sub>R overexpression led to major spatial memory alteration in tau transgenic mice: tau/A<sub>2A</sub>R did not exhibit preference for the target over the other quadrants ( $P = 0.76$ ), with a non-significant proportion of time in the target than expected by chance ( $33.5 \pm 6.2\%$ ,  $P = 0.22$ ). Tau/A<sub>2A</sub>R mice also spent less time in the target quadrant as compared to tau transgenic mice ( $P = 0.07$ ) and wild-type animals ( $P < 0.01$ ; Fig. 3E). Moreover, while the latency to reach the target hole was similar in wild-type, A<sub>2A</sub>R and tau mice, it was significantly enhanced in tau/A<sub>2A</sub>R animals ( $P < 0.01$  versus wild-type; Fig. 3F). Altogether, behavioural evaluations indicate that neuronal A<sub>2A</sub>R overexpression potentiates the development of early spatial memory deficits in THY-Tau22 mice.

## Impact of neuronal overexpression of A<sub>2A</sub>R on tau pathology in THY-Tau22 mice

THY-Tau22 mice exhibit progressive memory impairment in parallel with the development of hippocampal tau hyperphosphorylation and aggregation (Van der Jeugd *et al.*, 2013; Burnouf *et al.*, 2013). Because of low physiological expression in extra-striatal areas, A<sub>2A</sub>R immunostaining was not observed in the hippocampus of wild-type and tau animals (Supplementary Fig. 7); however, in tau/A<sub>2A</sub>R mice, A<sub>2A</sub>R immunostaining was particularly observed in neurons of the CA1 and dentate gyrus (DG)/hilus regions (Fig. 4A), which are the brain areas with highest human tau transgene expression and developing prominent tau pathology in THY-Tau22 mice (Schindowski *et al.*, 2006; Van der Jeugd *et al.*, 2013).

### Figure 2 Continued

remained undetectable in the hippocampus of wild-type animals. Doxycycline treatment from mating to P28 (P28 w/ Dox, *middle*) abolished A<sub>2A</sub>R overexpression. Doxycycline removal from P28 promoted hippocampal A<sub>2A</sub>R overexpression in the latter animals as exemplified in 6 month-old animals i.e. 5 months after doxycycline removal (*right*). (C) A<sub>2A</sub>R immunostaining by immunohistochemistry under the same experimental conditions showing expression of the receptor in animals treated (*middle*) or not with doxycycline (*left*) as well as receptor re-expression following doxycycline withdrawal (*right*). Upper panels represent immunostainings at the level of the striatum and lower panels at the level of the hippocampus and cortex. Scale bar = 1 mm. (D) Co-immunostainings with A<sub>2A</sub>R (red) and either neuronal (NeuN), microglial (Iba1) or astrocytic (GFAP and S100β) markers (green) showing the neuronal-specificity of A<sub>2A</sub>R overexpression in CaMKII-tTA/TRE-A<sub>2A</sub>R mice. DAPI (blue) represents cell nuclei. Scale bar = 20 μm. (E) Co-immunostainings between A<sub>2A</sub>R (red), NeuN (as marker of mature neurons, white) and doublecortin (DCX, as marker of immature neurons, green) in CaMKII-tTA/TRE-A<sub>2A</sub>R mice (A<sub>2A</sub>R). A<sub>2A</sub>R was not expressed in immature neurons. Scale bar = 100 μm. (F) Averaged time course of field excitatory postsynaptic potentials (fEPSP) after perfusion with SCH58261 (50 nM) for 30 min on hippocampal slices from wild-type and double CaMKII-tTA/TRE-A<sub>2A</sub>R transgenic mice ( $*P < 0.05$ ,  $n = 5$  per group). A<sub>2A</sub>R blockade significantly inhibited fEPSPs in double transgenic mice suggesting a gain of function of A<sub>2A</sub>R upon their overexpression, whereby A<sub>2A</sub>R exerts a tonic control on basal synaptic transmission, a phenomenon that is not observed in wild-type animals.

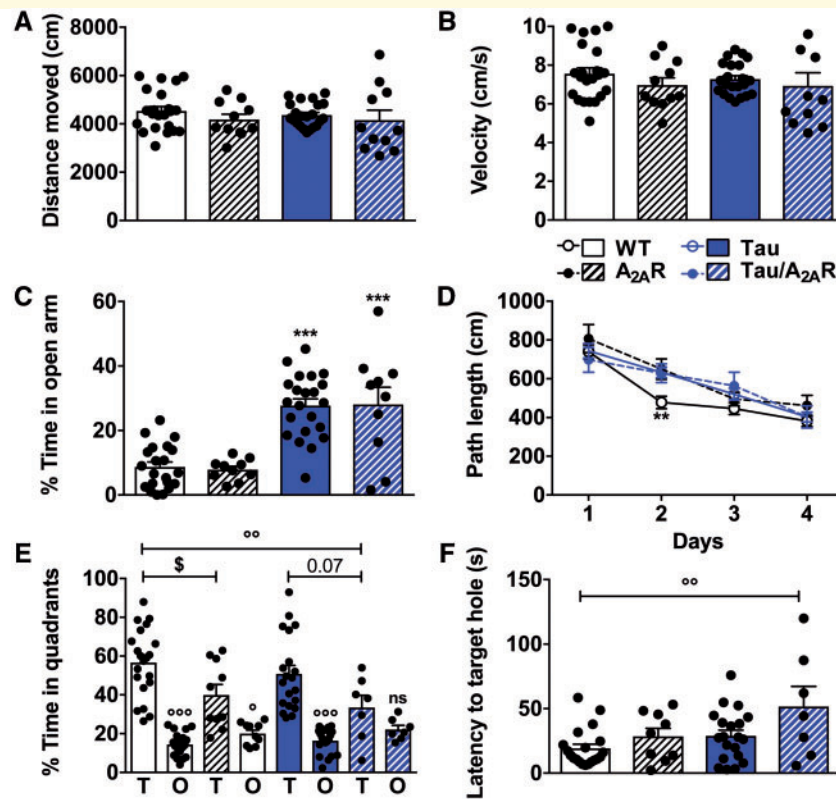


**Figure 3 Neuronal overexpression of  $A_{2A}R$  favours spatial memory deficits in THY-Tau22 transgenic mice.** Effects of neuronal overexpression of  $A_{2A}R$  on spontaneous activity, anxiety-like behaviour, spatial learning and memory of THY-Tau22 mice. **(A and B)** No change of either spontaneous locomotion or velocity was observed using actimetry. **(C)** Anxiety-like behaviour evaluated using elevated plus maze. Double transgenic mice overexpressing  $A_{2A}R$  performed as wild-type controls. As expected, tau transgenic mice spent more time in the open arms, a change similarly observed in triple tau/ $A_{2A}R$  transgenic mice. \*\*\* $P < 0.001$  versus wild-type mice using one-way ANOVA followed by Tukey's *post hoc* test. **(D)** Evaluation of the spatial learning using the Barnes maze task revealed that all groups of animals learned the position of the escape box in a time-dependent manner during the four days of training. **(E)** During the probe test, while displaying a preference,  $A_{2A}R$  mice spent significantly less time in the target quadrant (T) than wild-type controls. At the early age tested (5–6 months old), tau transgenic mice did not exhibit significant memory impairments with a strong preference for the target quadrant. In contrast, triple tau/ $A_{2A}R$  mice did not show preference for the target quadrant (T) over the other quadrants (O), supporting significant spatial memory deficits.  $^{\$}P < 0.05$  versus wild-type mice;  $^{\circ}P < 0.05$ ,  $^{\circ\circ}P < 0.01$ ,  $^{\circ\circ\circ}P < 0.001$  versus Target quadrant using one-way ANOVA followed by Tukey's *post hoc* test. **(F)** In agreement, the latency to reach the target hole was significantly increased for tau/ $A_{2A}R$  mice as compared to the other experimental groups.  $^{\circ\circ}P < 0.01$  versus wild-type mice using one-way ANOVA followed by Tukey's *post hoc* test.  $n = 7$ –22 per group. Results are expressed as mean  $\pm$  SEM.

This opened the possibility that increased neuronal  $A_{2A}R$  levels may accelerate the development of hippocampal tau pathology, thereby potentiating memory deficits in tau/ $A_{2A}R$  mice. We therefore compared levels of tau hyperphosphorylation and conformational changes in tau/ $A_{2A}R$  versus tau mice using biochemical and immunohistochemical approaches. In a first attempt, given the important number of phosphorylation sites on tau (Sergeant *et al.*, 2008), we performed a 2D gel electrophoresis analysis to evaluate global charge changes of human tau protein in the hippocampus of THY-Tau22 mice expressing or not the neuronal  $A_{2A}R$  transgene. As shown in Fig. 4B, we observed an increase of tau isoforms in the acidic pH range in tau/ $A_{2A}R$  mice as compared to tau mice, suggesting changes in global tau phosphorylation. We evaluated tau phosphorylation further in both experimental groups by western blot analyses using antibodies raised against selected tau phospho-epitopes. In line with the 2D analysis, we

observed a significant effect of  $A_{2A}R$  overexpression upon tau phosphorylation with a significant increase at S396 ( $+59.0 \pm 14.6\%$ ;  $P = 0.0044$  versus tau mice) and a reduction of dephosphorylated tau (tau-1 antibody recognizing S195/S198/S199/S202 dephosphorylated epitopes;  $-44.7 \pm 3.1\%$   $P = 0.01$  versus tau mice; Fig. 4C). We could neither detect changes at other phospho-epitopes including S212/T214 (AT100), nor changes in tau proteolysis (Fig. 4C). Moreover, immunohistochemical evaluation of tau pathology using MC1 conformational antibody did not show a difference between the tau and tau/ $A_{2A}R$  groups (Fig. 4D). Of note, we could not evidence tau phosphorylation changes in wild-type mice overexpressing  $A_{2A}R$  (Supplementary Fig. 8). To address potential mechanisms explaining changes in tau phosphorylation, we evaluated the protein level and/or phosphorylation of several kinases known to be involved in the phosphorylation of the modified epitopes: p38, CK2,

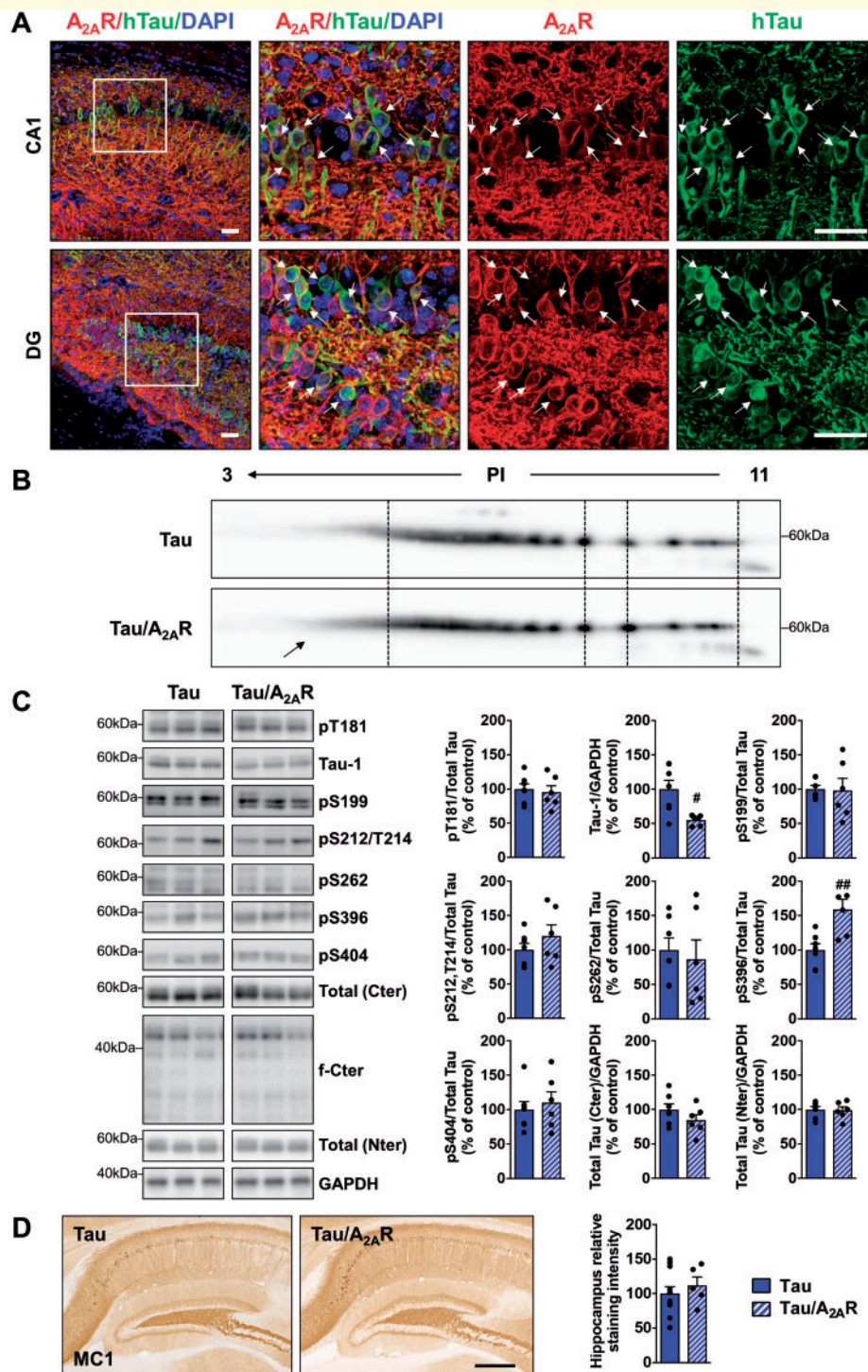


**Figure 4 Impact of neuronal A<sub>2A</sub>R overexpression on hippocampal tau pathology.** Human tau expression, phosphorylation and aggregation in the hippocampus of triple transgenic mice (tau/A<sub>2A</sub>R) versus tau transgenic controls were evaluated by immunohistochemistry, bidimensional electrophoresis (2D) and western blots. **(A)** Co-immunostainings with A<sub>2A</sub>R (red) and human tau (TauE1E2 antibody, human total tau, green) in the CA1 and dentate gyrus (DG) regions of triple tau/A<sub>2A</sub>R transgenic mice. Neurons expressing human tau transgene (arrows) were found to overexpress A<sub>2A</sub>R. DAPI (blue) represents cell nuclei. Scale bar = 50 μm. **(B)** 2D profile of total human tau (Cter antibody) in triple tau/A<sub>2A</sub>R mice and littermate tau controls, shows an increase of tau isovariants in the acidic range of PI (arrow). **(C)** Quantification of tau phosphorylation at T181, S199, S212/T214 (AT100), S262, S396 and S404 epitopes, as well as dephosphorylated tau (tau-1) in triple tau/A<sub>2A</sub>R animals and littermates tau controls. Analysis revealed tau hyperphosphorylation in tau/A<sub>2A</sub>R mice signed by increased pS396 and reduced tau-1 (dephosphorylated tau). \**P* < 0.05, \*\*\**P* < 0.01 versus tau mice using Student's *t*-test. *n* = 6–7 per group. **(D)** Conformational tau immunostaining using MCI antibody in triple tau/A<sub>2A</sub>R animals and littermates tau controls revealed no difference between groups. *n* = 5–11 per group. Scale bar = 500 μm. Results are expressed as mean ± SEM.

GSK3 $\beta$ , JNK, ERK, cdk5 and its activator p35 (Sergeant *et al.*, 2018). We could observe a trend for an increased level of CK2 as well as a significant upregulation of p35 ( $P = 0.033$  in tau/ $A_{2A}R$  versus tau mice; Supplementary Fig. 9). In THY-Tau22 mice, tau pathology has previously been associated to the degeneration of cholinergic neurons of the medial septum, which has been linked to memory deficits (Belarbi *et al.*, 2009, 2011). As shown in Supplementary Fig. 10A, while we could readily observe the expected loss of cholinergic neurons in the medial septum of THY-Tau22 mice ( $P = 0.0037$  versus wild-type mice), the number of neurons was similar in tau/ $A_{2A}R$  animals ( $P = 0.97$ ). Accordingly, using western blot, we did not observe change in hippocampal ChAT levels between tau and tau/ $A_{2A}R$  animals, suggesting that receptor overexpression did not impact cholinergic terminals in tau transgenic mice (Supplementary Fig. 10B). Altogether, these data suggest that hippocampal neuronal overexpression of  $A_{2A}R$  does not exert a major impact upon cholinergic alterations induced by the development of tau pathology.

### Neuronal overexpression of $A_{2A}R$ promotes upregulation of a microglial transcriptomic signature in tau transgenic mice

To gain mechanistic insights on how neuronal  $A_{2A}R$  overexpression could affect memory abilities in tau transgenic mice, we performed RNA sequencing from the hippocampus of the different experimental groups at the age of 6 months. In line with our previous data (Chatterjee *et al.*, 2018), a limited number of differentially expressed genes was found in tau transgenic as compared to wild-type mice (two upregulated and one downregulated). Neuronal overexpression of  $A_{2A}R$  itself did not lead to transcriptomic changes (not shown). Strikingly, when compared to tau transgenic mice, neuronal overexpression of  $A_{2A}R$  in tau animals (tau/ $A_{2A}R$ ) led to 505 significantly differentially expressed genes ( $\log_2$  fold-change  $> 0.32$ ,  $P_{\text{adjusted}} < 0.05$ ), 64 being upregulated and 441 downregulated (Fig. 5A). Functional Biological Process annotations indicated that downregulated genes in tau/ $A_{2A}R$  mice showed an enrichment of genes associated with RNA metabolism (Supplementary Fig. 11A and B). Upregulated genes were associated with immune processes and innate immune response (Fig. 5B). Using the STRING database, we observed a strong interaction between 24 of 64 upregulated gene products, with a notable cluster related to immune processes (Fig. 5C). To gain more insight into the upregulated genes in tau/ $A_{2A}R$  animals, we evaluated the cell-specific enrichment of these genes using a CNS RNA-seq database generated by the laboratory of Ben Barres (Zhang *et al.*, 2014; [http://web.stanford.edu/group/barres\\_lab/brain\\_rnaseq.html](http://web.stanford.edu/group/barres_lab/brain_rnaseq.html)). Interestingly, while  $A_{2A}R$  upregulation is experimentally induced in a cell-specific manner in the hippocampal neurons of tau/ $A_{2A}R$  mice, we found that few of the 54 upregulated genes annotated in the database were enriched in neurons. Rather, and in line with the association of these genes with immune-related processes, 33 of these

upregulated 54 genes (~61%) were enriched in microglia (Fig. 5D). Among these genes were *Csf1r*, *Trem2* and *C1qa*, which we validated by quantitative PCR experiments from additional hippocampal mRNA samples (Fig. 6A and Supplementary Fig. 11C). Recent microglia-specific RNA-seq studies found that microglia in neurodegenerative diseases exhibit a transcriptional profile that is distinct from classical activation during infection (Butovsky and Weiner, 2018). We compared the set of 33 microglia-enriched upregulated genes in tau/ $A_{2A}R$  mice with microglial transcriptional profiles from these studies but found only limited overlap (Holtman *et al.*, 2015; Keren-Shaul *et al.*, 2017; Mathys *et al.*, 2017), possibly due to technical differences in analysis (whole tissue versus microglia-specific analysis). However, we found considerable overlap between microglial upregulated genes in tau/ $A_{2A}R$  mice with upregulated genes in the PS2APP mouse model of cerebral amyloidosis (26 similar genes) and SOD1 mouse model of familial amyotrophic lateral sclerosis (25 similar genes), both derived from whole-tissue analyses (cortex or spinal cord) (Srinivasan *et al.*, 2016), suggesting that tau/ $A_{2A}R$  mice exhibit gene expression alterations that have previously been linked to neurodegeneration.

In addition to their transcriptional response, microglia typically increase in cell number and considerably change their morphology during ageing and neurodegenerative disease (Baron *et al.*, 2014), reflective of an altered activation status and functional changes, e.g. in phagocytosis. On the other hand, limited morphological alterations were found in microglia in early stages of cerebral amyloidosis despite an increase in microglial phagocytosis of synaptic material (Hong *et al.* 2016), suggesting that morphology alterations are not a prerequisite for microglia functional changes. To characterize cell number and morphology changes in wild-type,  $A_{2A}R$ , tau and tau/ $A_{2A}R$  mice, we analysed Iba1-immunolabeled microglia in the CA1 and dentate gyrus regions. To this end, we used custom-written ImageJ plugins, which allow the automated quantification of cell somata in 3D tissue and the 3D reconstruction and cell skeleton analysis of a high number of individual microglial cells (Fig. 5E; Plescher *et al.*, 2018). Overall, we found no significant cell number changes in the four analysed mouse groups (Fig. 5F and G). Furthermore, microglial morphological parameters e.g. ramification index (a measure for cellular complexity), spanned volume (a measure for the CNS volume surveilled by one microglial cell) and total dendritic tree length (a measure for the complexity of cell skeleton) did not differ significantly between the groups (Fig. 5F and G).

### Neuronal overexpression of $A_{2A}R$ in tau mice promotes hippocampal C1q upregulation and synaptic loss in the dentate gyrus

Previous work has underlined the involvement of C1q in age-related cognitive decline and synaptic loss in

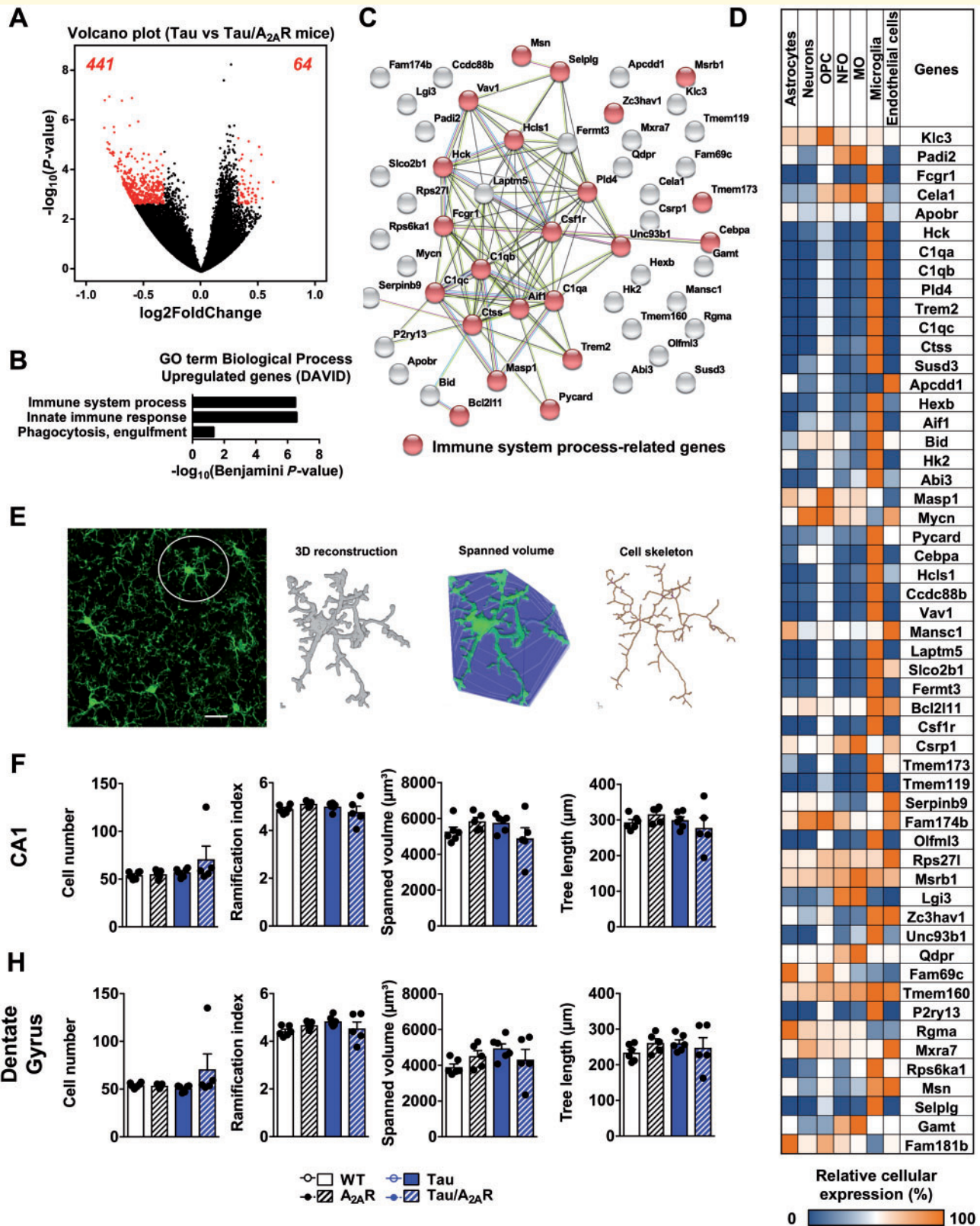


**Figure 5** Neuronal overexpression of A<sub>2A</sub>R promotes the upregulation of a microglial transcriptomic signature in the hippocampus of tau transgenic mice. RNA sequencing analysis of the hippocampus of wild-type, double A<sub>2A</sub>R, tau and triple tau/A<sub>2A</sub>R animals at the age of 6 months ( $n = 4$  per genotype). **(A)** Volcano plot showing the 505 genes differentially regulated genes between tau/A<sub>2A</sub>R mice and tau mice. Red dots represent significantly dysregulated genes with log<sub>2</sub> fold change > 0.32 and adjusted  $P$ -value < 0.05. Sixty-four genes were found significantly upregulated (right) and 441 significantly downregulated (left). **(B)** Functional annotation of the 64 upregulated genes in the triple tau/A<sub>2A</sub>R mice versus tau was performed with DAVID for GOTERM\_Biological Process and showed a significant association with immune

(continued)

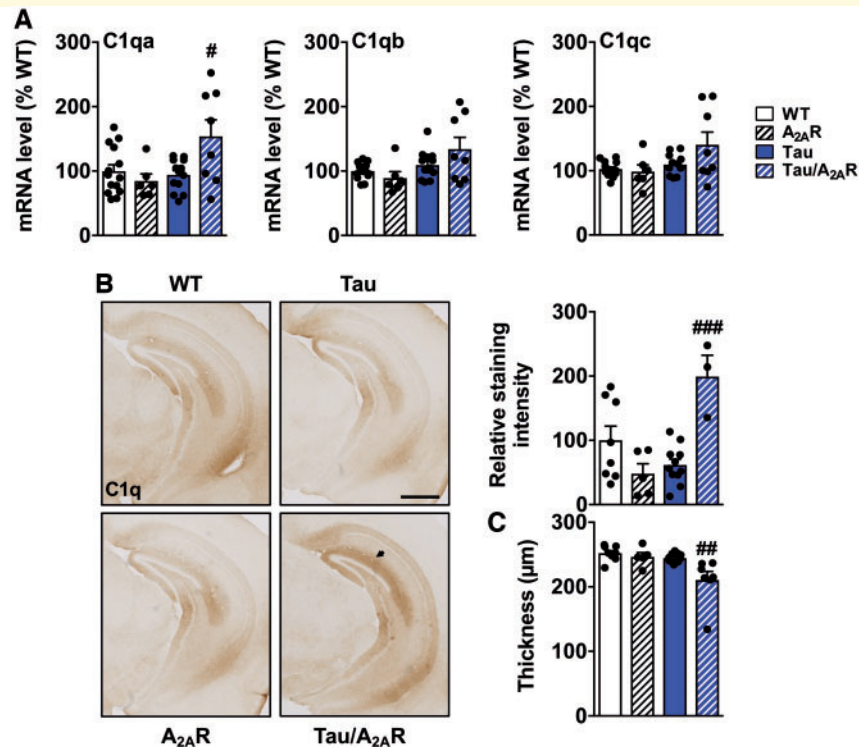


**Figure 6** Neuronal overexpression of A<sub>2A</sub>R in tau mice is associated with upregulation of C1q and hippocampal atrophy.

(A) Independent, quantitative PCR analysis of *C1qa*, *C1qb* and *C1qc*, the three genes encoding for functional heterotrimeric C1q protein.  $^{\#}P < 0.05$  versus tau mice using one-way ANOVA followed by Tukey's *post hoc* test.  $n = 6$ –14 per group. (B) Representative images of anti-C1q immunohistochemistry and related quantification showing an upregulation of C1q immunoreactivity in the hippocampus of tau/A<sub>2A</sub>R mice, with a particular intense signal in the dentate gyrus (DG, arrow). Scale bar = 1 mm.  $^{###}P < 0.001$  versus tau mice using one-way ANOVA followed by Tukey's *post hoc* test.  $n = 3$ –11 per group. (C) Morphometric analysis of dentate gyrus thickness in the hippocampus of all experimental groups  $^{\#}P < 0.05$ ,  $^{##}P < 0.01$  versus tau mice using one-way ANOVA followed by Tukey's *post hoc* test.  $n = 5$ –11 per group.

Alzheimer's disease and tauopathies (Stephan *et al.*, 2013; Hong *et al.*, 2016; Dejanovic *et al.*, 2018). While hippocampal mRNA and protein levels of C1q were found to be similar in wild-type, A<sub>2A</sub>R and tau transgenic mice, they were significantly upregulated in tau/A<sub>2A</sub>R animals as compared to tau mice (Fig. 6A and B), with a notable increase in the molecular layer of the dentate gyrus (Fig. 6B), associated to a significant atrophy of this hippocampal area in tau/A<sub>2A</sub>R animals ( $-13.8 \pm 5.4\%$  versus tau mice;  $P < 0.01$ ; Fig. 6C). A time-course evaluation of C1q mRNA

expression indicated that C1q upregulation in the hippocampus in THY-Tau22 mice occurs only from 9 months of age onwards (Supplementary Fig. 12A), which—interestingly—is the time point when these mice exhibit memory alterations (Van der Jeugd *et al.*, 2013; Laurent *et al.*, 2016, 2017) and dendritic spine alterations (Burlot *et al.*, 2015; Chatterjee *et al.*, 2018). This observation suggested that early neuronal overexpression of A<sub>2A</sub>R in tau transgenic mice led to an accelerated phenotype in THY-Tau22 mice. Further, corroborating the link between tau

#### Figure 5 Continued

system processes, innate immune response and phagocytosis engulfment. (C) Known and predicted protein interaction (STRING) of the genes belonging to the significant GO term processes shown in C. (D) Heat map representing the cellular enrichment of each upregulated gene based on a transcriptome database of purified populations of neurons, astrocytes, oligodendrocyte precursor cells (OPC), newly formed oligodendrocytes (NFO), myelinating oligodendrocytes (MO), microglia and endothelial cells (Zhang *et al.*, 2014). Relative cellular enrichment of each gene is given as the percentage of highest expression. Expression of 54 out of the 64 genes upregulated was knowledgeable in the database. Among these 54 genes, 33 were particularly enriched in microglial cells, contrasting with the lack of neuronal enrichment. (E) Cell number and cell morphology of Iba1-immunolabeled microglia (green) were analysed in confocal images using custom-written ImageJ plugins. A representative confocal image, the 3D reconstruction, visualization of spanned volume and cell skeleton derived from one representative cell in the confocal image are shown. (F and G) Quantification of microglia cell number and the morphological parameters ramification index, spanned volume and total tree length of cell skeleton revealed no difference between the mouse groups in the CA1 (F) or dentate gyrus (G) regions.  $n = 5$ –6 mice per genotype. Results are expressed as mean  $\pm$  SEM. Scale bar = 20  $\mu$ m.

pathology, A<sub>2A</sub>R and C1q, we found that neuronal upregulation of A<sub>2A</sub>R in FTL D patients with P301L *MAPT* mutation correlated with an increased C1q expression (Fig. 7). Interestingly, we also observed C1q and A<sub>2A</sub>R

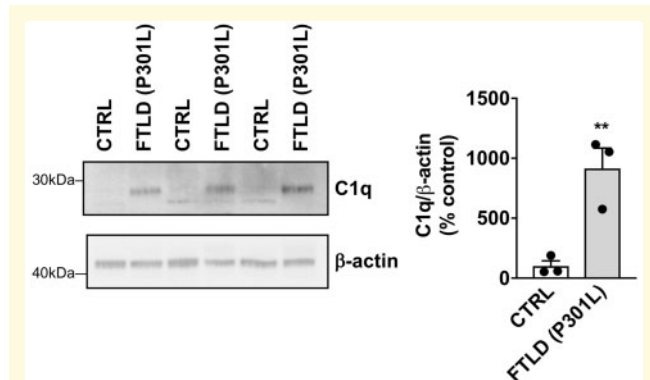


**Figure 7** C1q upregulation in the temporal cortex of patients with frontotemporal dementia (FTLD-tau) carrying P301L mutations. Western blot analysis of C1q levels in the cortex of FTLD-tau patients and age-matched controls (CTRL) revealing a significant increase in tauopathic patients.  $**P < 0.01$  versus Control using Student's *t*-test.  $n = 3$  per group.

upregulations in the frontal cortex of patients with two other forms of FTLD-tau without *MAPT* mutation i.e. CBD and Pick's disease (Supplementary Fig. 12B and C). Finally, using immunohistochemistry for the inhibitory and excitatory presynaptic markers VGAT and VGLUT1 (Fig. 8A), we found that the density of VGLUT1-immunoreactive synapses was significantly reduced in the molecular layer (Fig. 8B)—but not in the hilus (Fig. 8D)—of tau/A<sub>2A</sub>R mice as compared to tau animals ( $P < 0.05$ ). In contrast, the number of VGAT-immunoreactive synapses was unaffected (Fig. 8C), suggesting a specific loss of glutamatergic synapses in tau/A<sub>2A</sub>R animals. Altogether, these data suggest that the overexpression of A<sub>2A</sub>R in neurons of tau transgenic mice drives C1q upregulation and a loss of glutamatergic synapses in the dentate gyrus.

## Discussion

Here, we report the first evidence that early neuronal upregulation of A<sub>2A</sub>R potentiates tau-dependent memory deficits, suggesting an instrumental role of A<sub>2A</sub>R dysregulation in the development of cognitive decline in Alzheimer's disease and tauopathies.

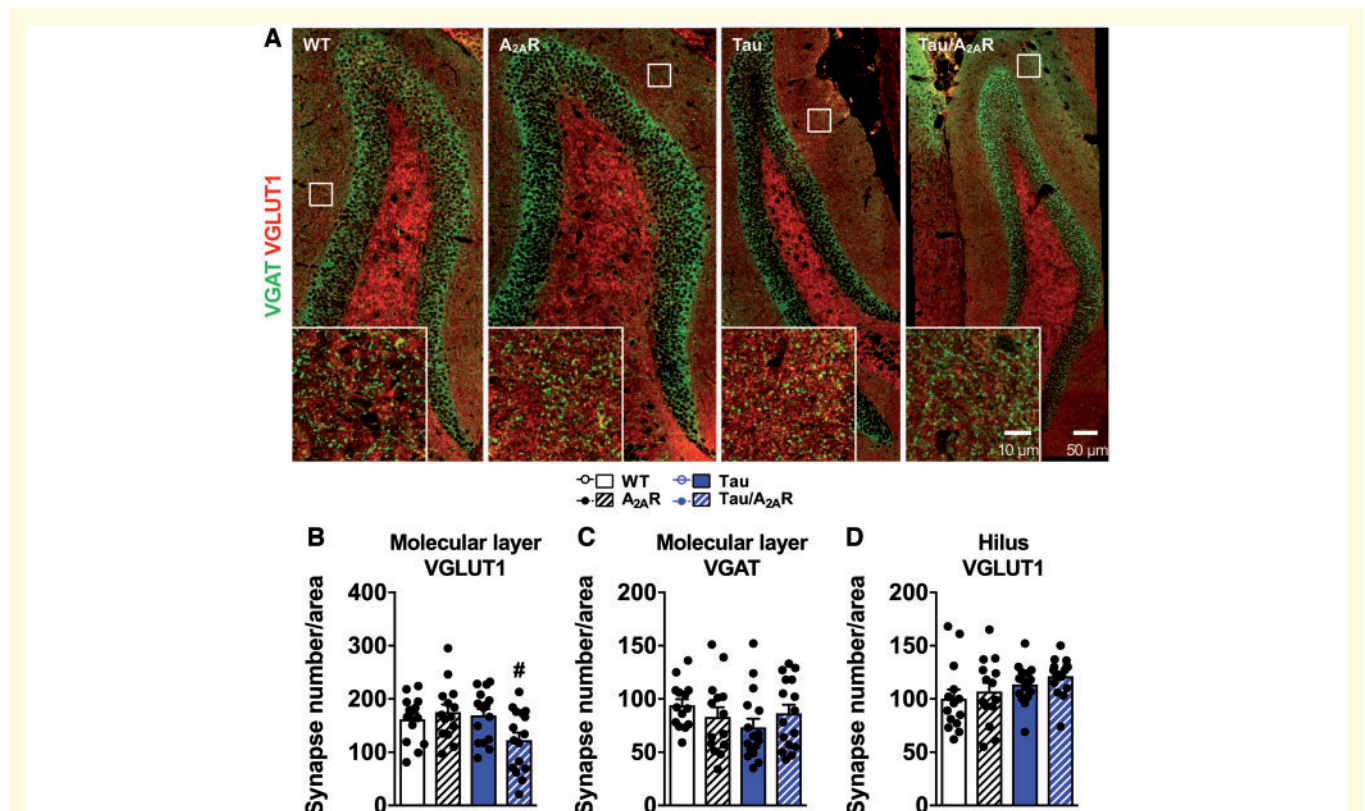


**Figure 8** Neuronal overexpression of A<sub>2A</sub>R in tau mice is associated with synaptic loss. (A) Characteristic immunofluorescence for inhibitory and excitatory presynaptic markers VGAT (green) and VGLUT1 (red) in the dentate gyrus from wild-type, A<sub>2A</sub>R, tau and tau/A<sub>2A</sub>R mice, at low (scale bar = 50  $\mu$ m) and higher magnification (inset, scale bar = 10  $\mu$ m). A marked decrease in VGLUT1 but not VGAT immunoreactivity was observed in the molecular layer of the dentate gyrus of tau/A<sub>2A</sub>R mice. The total number of VGLUT1 synapses per area was decreased in tau/A<sub>2A</sub>R mice in the molecular layer (B) but not in the hilus (D). VGAT synapses remained unaffected in the molecular layer (C).  $\#P < 0.05$  versus tau mice using one-way ANOVA followed by Tukey's *post hoc* test,  $n = 14$ –16 images from four mice per group. Results are expressed as mean  $\pm$  SEM.

A<sub>2A</sub>R has been described to act as a fine tuner of synaptic plasticity (Cunha, 2016) and its cortical and hippocampal dysregulation has been associated with several cognitively unfavourable conditions such as ageing (Lopes *et al.*, 1999; Canas *et al.*, 2009a; Temido-Ferreira *et al.*, 2018) or neurodegenerative and neuropsychiatric disorders (Cunha, 2016), such as chronic stress (Batalha *et al.*, 2013; Kaster *et al.*, 2015) and Alzheimer's disease (Albasanz *et al.*, 2008; Temido-Ferreira *et al.*, 2018). Regarding Alzheimer's disease, A<sub>2A</sub>R dysregulation in neurons or astrocytes has been linked to amyloid pathology (Viana da Silva *et al.*, 2016; Faivre *et al.*, 2018; Lee *et al.*, 2018; Orr *et al.*, 2018). Our current observation of an A<sub>2A</sub>R upsurge in the cortex of patients with FTLD-tau with or without *MAPT* mutations (FTLD-tau with P301L mutation, CBD and Pick's disease) also links A<sub>2A</sub>R dysregulation with tau pathology, which is consistent with previous data reporting A<sub>2A</sub>R density increase in ageing, when tau pathology is present (Temido-Ferreira *et al.*, 2018) and in a tauopathy, Pick's disease (Albasanz *et al.*, 2006).

To address a potential link between A<sub>2A</sub>R and tau pathology, we developed a new transgenic mouse model allowing the postnatal overexpression of A<sub>2A</sub>R in forebrain neurons of the THY-Tau22 mouse model, a tauopathy model based on FTLD *MAPT* mutations. We elicited A<sub>2A</sub>R neuronal upregulation from 1 month onward, i.e. before the onset of hippocampal tau pathology (2–3 months of age), and evaluated the consequences at 5–6 months of age, when tau transgenic animals normally exhibit ongoing tau pathology with minimal memory impairments (Van der Jeugd *et al.*, 2013). Strikingly, spatial memory was strongly decreased in tau mice overexpressing neuronal A<sub>2A</sub>R. Interestingly, associated with memory loss, we found global changes of tau phosphorylation using 2D electrophoresis and >50% increased hyperphosphorylation at S396 and S195/S198/S199/S202 in tau/A<sub>2A</sub>R animals as compared to tau littermates. These alterations are in the range of the phosphorylation changes associated with the development of memory deficits in this mouse strain (Schindowski *et al.*, 2006). Further, similar variations in magnitude have been found associated with changes in the memory abilities of THY-Tau22 mice in our previous works (Leboucher *et al.*, 2013; Laurent *et al.*, 2016). Since A<sub>2A</sub>R overexpression and human tau transgene co-localized in hippocampal neurons, such changes in tau phosphorylation could be ascribed to neuron-autonomous changes. While underlying mechanisms remain to be uncovered, we could notably observe a significant increase in p35, known to favour the activation of cdk5, an important tau kinase (for review see Hamdane and Buee, 2007).

Our data raise the question of the temporal interconnection between A<sub>2A</sub>R dysregulation and tau hyperphosphorylation: which comes first? From what we know about Alzheimer's disease and aged individuals, it is clear that both tau pathology and A<sub>2A</sub>R receptor upregulation occur early, failing to resolve the temporal hierarchy between the two. When we compared tau phosphorylation

in wild-type animals overexpressing A<sub>2A</sub>R or not, we could not observe changes in tau phosphorylation. This suggests that in pathological conditions such as Alzheimer's disease and tauopathies, A<sub>2A</sub>R upregulation occurs secondary, also in line with previous works (Viana da Silva *et al.*, 2016; Silva *et al.*, 2018; Temido-Ferreira *et al.*, 2018). Interestingly, synaptic A<sub>2A</sub>R upregulation has been observed in several neuro-psychiatric conditions, which are not considered as tauopathies, for instance chronic stress, seizures and depression (i.e. Kaster *et al.*, 2015; Machado *et al.*, 2017; Canas *et al.*, 2018). Encompassing more than 80 phosphorylation sites targeted by more than 30 kinases (Sergeant *et al.*, 2008), tau could be viewed as a homeostatic protein, like A<sub>2A</sub>R, which can be modulated in detrimental situations. In line, previous work reported tau hyperphosphorylation in conditions eliciting A<sub>2A</sub>R synaptic upregulation such as stress or epilepsy (Lopes *et al.*, 2016; Machado *et al.*, 2019). Therefore, the sole increase of A<sub>2A</sub>R alone is not sufficient to promote tau hyperphosphorylation. Rather, a parenchymal dyshomeostasis such as ageing or chronic excitability changes is required. In the latter situation, the co-occurrence of A<sub>2A</sub>R upregulation and tau hyperphosphorylation, as we experimentally induced in tau/A<sub>2A</sub>R animals, would then exacerbates tau pathology and these dyshomeostatic processes, in a detrimental loop.

Such potentiating effect of A<sub>2A</sub>R overexpression in tau transgenic mice is particularly supported by our RNA-seq data. As compared to controls, A<sub>2A</sub>R neuronal upregulation alone in a wild-type background did not elicit basal transcriptomic changes, suggesting a post-transcriptional basis for the memory alteration in A<sub>2A</sub>R-overexpressing animals, consistent with the aberrant A<sub>2A</sub>R/NMDA/mGluR5 interplay we recently described in a rat model of constitutive neuronal A<sub>2A</sub>R overexpression (Temido-Ferreira *et al.*, 2018). Further, at 6 months of age, basal transcriptomic changes in the hippocampus of tau transgenic mice were marginal with only three genes significantly affected (*Thy1*, *Ccl6* and *Mvd*). In sharp contrast, A<sub>2A</sub>R upregulation in a tau background led to a significant change in the expression of 505 genes. Interestingly, the upregulation of A<sub>2A</sub>R in hippocampal neurons at an early pathological stage of tau mice elicited a singular response of genes enriched in microglia. This immune-related gene expression profile showed a considerable overlap with transcriptomic profiles found in other neurodegenerative diseases (Srinivasan *et al.*, 2016), but was different from the inflammatory signature elicited by tau pathology itself at later stages in the THY-Tau22 mouse model (Laurent *et al.*, 2017; Chatterjee *et al.*, 2018). Interestingly, microglial number and morphology were not significantly altered in tau/A<sub>2A</sub>R mice, similar to what has been described in early stages of cerebral amyloidosis (Hong *et al.*, 2016). Besides the link between neuronal tau hyperphosphorylation and microglial C1q changes (see below), we were also interested in other potential changes that could cause alteration of neuro-microglia communication that may occur in

the hippocampus of tau/A<sub>2A</sub>R animals and potentially explain plasticity changes. It is recognized that there is a bidirectional communication between neurons and microglia, involving several systems such as CX3CL1/CX3CR1, TGFβ/TGFβR, CSF1/CSF1R, ATP/P2X7 and CD200/CD200 (Wohleb, 2016). Using our RNA-seq data, we have then checked individual expression of several genes involved in neuron-microglia communication. As seen in Supplementary Fig. 13, comparing RPKM values (reads per kilobase of transcript per million mapped), the only markers we found to be changed in tau/A<sub>2A</sub>R versus tau animals were CSF1R, which were validated as upregulated by quantitative PCR (Supplementary Fig. 11) as well as CSF1 and CX3CR1, which could not be further validated by quantitative PCR (data not shown). Our observations therefore underline a possible modification of neuro-microglia communication via CSF1/CSF1R in tau/A<sub>2A</sub>R animals. Previous studies demonstrated an association between brain injury and neuronal CSF1 upregulation (Luo *et al.*, 2013; Guan *et al.*, 2016; Wohleb *et al.*, 2018). Notably, Wohleb *et al.* (2018) demonstrated that engagement of the CSF1/CSF1R system in chronic stress favours dendritic remodelling and stress-induced behavioural deficits. Changes in CSF1R uncovered in tau/A<sub>2A</sub>R animals may therefore contribute to the cognitive phenotype we observed.

Among all markers uncovered in tau/A<sub>2A</sub>R animals, and despite the potential involvement of RNA-related pathways found downregulated, we particularly focused our interest on C1q. C1q is the initiator component of the classical complement pathway, which is predominantly expressed by microglial cells (Fonseca *et al.*, 2017) and physiologically plays a major role in synapse pruning during development (Schafer *et al.*, 2012). Our RNA sequencing analysis revealed that the neuronal upregulation of A<sub>2A</sub>R in tau mice—which promotes spatial memory alterations—is associated with hippocampal upregulation of the mRNAs encoding the three polypeptide chains composing C1q complement protein complex i.e. *C1qa*, *C1qb* and *C1qc*. Increased expression of C1q was confirmed by immunohistochemistry. Notably, A<sub>2A</sub>R upregulation in wild-type mice was insufficient to promote C1q increase, an observation confirmed in a rat model, constitutively overexpressing A<sub>2A</sub>R in forebrain neurons (data not shown; Temido-Ferreira *et al.*, 2018).

Hippocampal C1q upregulation has been observed in the brain of mouse models or individuals with viral infection (Vasek *et al.*, 2016), during ageing (Stephan *et al.*, 2013) or Alzheimer's disease (Fonseca *et al.*, 2004; Hong *et al.*, 2016; Dejanovic *et al.*, 2018), which are all characterized by memory impairments. The causal link between C1q upsurge and cognitive dysfunction promoted by ageing or cerebral amyloidosis has been established by the observation that C1q deletion or blockade restored plasticity and memory (Stephan *et al.*, 2013; Hong *et al.*, 2016). Along the same line, memory and plasticity improvement of PS19 tau mice upon deletion of TYROBP, an adaptor protein for TREM2, has been linked to C1q downregulation

(Audrain *et al.*, 2018). In Alzheimer's disease, cognitive deficits are correlated to synaptic loss (Spires-Jones and Hyman, 2014). Recent reports suggest a reactivation of the complement pathway in neurodegenerative conditions (Hong *et al.*, 2016; Dejanovic *et al.*, 2018). Notably, amyloid-β and tau were found to promote the synaptic tagging by C1q and the subsequent engulfment by microglial cells (Hong *et al.*, 2016; Dejanovic *et al.*, 2018). Interestingly, our data indicate that in tau/A<sub>2A</sub>R animals, memory impairment is associated with synaptic loss in the molecular layer of the dentate gyrus, which exhibited the highest rise of C1q. Only VGLUT1, and not VGAT, synapses were lost, in accordance with the particular vulnerability of excitatory synapses to C1q as recently reported in the PS19 tau transgenic model (Dejanovic *et al.*, 2018). Moreover, our time course analysis of C1q expression in the THY-Tau22 model (Supplementary Fig. 12A) indicates that C1q is not upregulated before tau mice reach 9 months of age, a time point where these animals exhibit major memory alterations and spine degeneration (Burlot *et al.*, 2015; Chatterjee *et al.*, 2018). These data, together with our observations in different forms of FTLT-tau, suggest that C1q upregulation follows neuronal tau hyperphosphorylation, leading to synaptic degeneration. This idea is consistent with the recent findings by Dejanovic *et al.* (2018), which demonstrated a correlation between the tau pathological load (AT8), the synaptic tagging by C1q and the synapse loss in another, faster, tau transgenic mouse model (P301S). By overexpressing A<sub>2A</sub>R in THY-Tau22 mice, we therefore elicit, at an early time point (5–6 months of age), increased tau hyperphosphorylation, which is sufficient to promote a C1q upregulation and the associated synaptic loss seen normally at 9 months in THY-Tau22 mice. This is again well in line with findings by Dejanovic *et al.* (2018), which point toward a 'critical microglia-neuron interaction in the synapse loss of tauopathy'. Tau-driven changes elicited by A<sub>2A</sub>R overexpression could therefore promote a signal between neurons and microglia to recruit C1q to the synapses and/or allow expression of the neuronal C1q synaptic receptor, all of which being crucial to study in future experiments.

Finally, the present work, together with several converging sets of data, supports the importance of early synaptic A<sub>2A</sub>R dysregulation in Alzheimer's disease (Viana da Silva *et al.*, 2016; Silva *et al.*, 2018; Temido-Ferreira *et al.*, 2018), while the role of astrocytic A<sub>2A</sub> receptors, which may be involved at later stages (Matos *et al.*, 2012; Orr *et al.*, 2015; Paiva *et al.*, 2019) remains currently unclear. The respective roles of both neuronal and astrocytic A<sub>2A</sub>R during the Alzheimer's disease course deserve more ample investigations in the future. One last pending question is the role of the mechanisms involved in adenosine formation, notably by the catabolism of extracellular ATP through druggable ecto-5'-nucleotidase (CD73), to sustain the overactivation of A<sub>2A</sub>R in pathological conditions (Augusto *et al.*, 2013; Gonçalves *et al.*, 2019).

In conclusion, the present data support the view that neuronal dysregulation of A<sub>2A</sub>R in Alzheimer's disease is involved in the development of synaptic/memory deficits and, in line with several preclinical studies including ours (Canas *et al.*, 2009b; Laurent *et al.*, 2016; Viana da Silva *et al.*, 2016; Orr *et al.*, 2018; Silva *et al.*, 2018; Temido-Ferreira *et al.*, 2018), that limiting A<sub>2A</sub>R dysregulation represents a key approach to provide benefit against plasticity impairments, synaptic degeneration and cognitive decline in Alzheimer's disease and other tauopathies.

## Acknowledgements

We thank the TGE RMN THC (FR-3050, France) for antibody TauE1E2 epitope characterization. We thank the Animal Facility (F-59000 Lille, France) and Cyrille Degraeve, Caroline Declerck, Kim Letten, Yann Lepage, Benjamin Guerrin, Didier Montignies, Christian Meunier, Quentin Dekeyser, Laure Taquet and Romain Dehaynin for animal care. We thank Meryem Tardivel and Antonino Bongiovanni for their help on the Zeiss confocal microscope from the Photonic Microscopy Core BioImaging Center (BiCel). We also thank the Functional Exploration Platform (SFR DN2M, Université de Lille) where behavioural assessment was performed. We thank the patients and their families for participating in the present study. We thank Claude-Alain Maurage and Vincent Deramecourt (Lille Neurobank), Charles Duyckaerts (NeuroCEB; GIE Neuro-CEB BB-0033-00011) and Eniko Kovari (HUG Brain bank) for providing and analysing the brain tissue samples. Sequencing was performed by the GenomEast Platform, a member of the 'France Génomique' consortium (ANR-10-INBS-0009).

## Funding

This work was supported by grants from Hauts-de-France (PARTEN-AIRR, COGNADORA), ANR (ADORATAU to D.B.) and Programs d'Investissements d'Avenir LabEx (excellence laboratory) DISTALZ (Development of Innovative Strategies for a Transdisciplinary approach to ALzheimer's disease). Our laboratories are also supported by ANR (GRAND, SPREADTAU to LB, ADORASTRAU to D.B.), Fondation pour la Recherche Médicale, France Alzheimer/Fondation de France, FHU VasCog research network (Lille, France), Fondation Vaincre Alzheimer, Fondation Plan Alzheimer as well as Inserm, CNRS, Université Lille, Lille Métropole Communauté Urbaine, DN2M. K.C. holds a doctoral grant from Lille University. V.G.-M. was supported by Fondation pour la Recherche Médicale (SPF20160936000). C.M. is supported by Région Hauts-de-France. X.M. and S.L. are funded by ANR (ADONIS), Fondation pour la Recherche Médicale et Fondation pour la Recherche sur le Cerveau. A.L.B. is supported by CNRS, Unistra, ANR-16-CE92-0031 (EPIFUS), Alsace Alzheimer

67, France Alzheimer (AAP SM 2017 #1664). L.V.L. and J.E.C. are funded by Fundação para a Ciência e Tecnologia (PTDC/4778/2014).

## Competing interests

The authors declare no conflict of interest.

## Supplementary material

Supplementary material is available at *Brain* online.

## References

- Albasanz JL, Perez S, Barrachina M, Ferrer I, Martín M. Up-regulation of adenosine receptors in the frontal cortex in Alzheimer's disease. *Brain Pathol* 2008; 18: 211–9.
- Albasanz JL, Rodríguez A, Ferrer I, Martín M. Adenosine A<sub>2A</sub> receptors are up-regulated in Pick's disease frontal cortex. *Brain Pathol* 2006; 16: 249–55.
- Anders S, Huber W. Differential expression analysis for sequence count data. *Genome Biol* 2010; 11: R106.
- Anders S, Pyl PT, Huber W. HTSeq—a Python framework to work with high-throughput sequencing data. *Bioinformatics* 2015; 31: 166–9.
- Audrain M, Haure-Mirande J-V, Wang M, Kim SH, Fanutza T, Chakrabarty P, et al. Integrative approach to sporadic Alzheimer's disease: deficiency of TYROBP in a tauopathy mouse model reduces C1q and normalizes clinical phenotype while increasing spread and state of phosphorylation of tau. *Mol Psychiatry* 2018.
- Augusto E, Matos M, Sévigny J, El-Tayeb A, Bynoe MS, Müller CE, et al. Ecto-5'-nucleotidase (CD73)-mediated formation of adenosine is critical for the striatal adenosine A<sub>2A</sub> receptor functions. *J Neurosci* 2013; 33: 11390–9.
- Balducci C, Santamaria G, La Vitola P, Brandi E, Grandi F, Viscomi AR, et al. Doxycycline counteracts neuroinflammation restoring memory in Alzheimer's disease mouse models. *Neurobiol Aging* 2018; 70: 128–39.
- Baron R, Babcock AA, Nemirovsky A, Finsen B, Monsonogo A. Accelerated microglial pathology is associated with A $\beta$  plaques in mouse models of Alzheimer's disease. *Aging Cell* 2014; 13: 584–95.
- Batalha VL, Ferreira DG, Coelho JE, Valadas JS, Gomes R, Temido-Ferreira M, et al. The caffeine-binding adenosine A<sub>2A</sub> receptor induces age-like HPA-axis dysfunction by targeting glucocorticoid receptor function. *Sci Rep* 2016; 6: 31493.
- Batalha VL, Pego JM, Fontinha BM, Costenla AR, Valadas JS, Baqi Y, et al. Adenosine A(2A) receptor blockade reverts hippocampal stress-induced deficits and restores corticosterone circadian oscillation. *Mol Psychiatry* 2013; 18: 320–31.
- Belarbi K, Burnouf S, Fernandez-Gomez F-J, Desmercières J, Troquier L, Brouillette J, et al. Loss of medial septum cholinergic neurons in THY-Tau22 mouse model: what links with tau pathology? *Curr Alzheimer Res* 2011; 8: 633–8.
- Belarbi K, Schindowski K, Burnouf S, Caillierez R, Grosjean M-E, Demeyer D, et al. Early Tau pathology involving the septo-hippocampal pathway in a Tau transgenic model: relevance to Alzheimer's disease. *Curr Alzheimer Res* 2009; 6: 152–7.
- Benjamini Y, Hochberg Y. Controlling the false discovery rate: a practical and powerful approach to multiple testing. *J R Stat Soc: Series B (Methodological)* 1995; 57: 289–300.
- Blum D, Chtarto A, Tenenbaum L, Brotchi J, Levivier M. Clinical potential of minocycline for neurodegenerative disorders. *Neurobiol Dis* 2004; 17: 359–66.

- Blum D, Hourez R, Galas M-C, Popoli P, Schiffmann SN. Adenosine receptors and Huntington's disease: implications for pathogenesis and therapeutics. *Lancet Neurol* 2003; 2: 366–74.
- Burgin KE, Waxham MN, Rickling S, Westgate SA, Mobley WC, Kelly PT. In situ hybridization histochemistry of Ca<sup>2+</sup>/calmodulin-dependent protein kinase in developing rat brain. *J Neurosci* 1990; 10: 1788–98.
- Burlot M-A, Braudeau J, Michaelsen-Preusse K, Potier B, Ayciriex S, Varin J, et al. Cholesterol 24-hydroxylase defect is implicated in memory impairments associated with Alzheimer-like Tau pathology. *Hum Mol Genet* 2015; 24: 5965–76.
- Burnouf S, Martire A, Derisbourg M, Laurent C, Belarbi K, Leboucher A, et al. NMDA receptor dysfunction contributes to impaired brain-derived neurotrophic factor-induced facilitation of hippocampal synaptic transmission in a Tau transgenic model. *Aging Cell* 2013; 12: 11–23.
- Butovsky O, Weiner HL. Microglial signatures and their role in health and disease. *Nat Rev Neurosci* 2018; 19: 622–35.
- Canas PM, Duarte JMN, Rodrigues RJ, Köfalvi A, Cunha RA. Modification upon aging of the density of presynaptic modulation systems in the hippocampus. *Neurobiol Aging* 2009a; 30: 1877–84.
- Canas PM, Porciúncula LO, Cunha GMA, Silva CG, Machado NJ, Oliveira JMA, et al. Adenosine A<sub>2A</sub> receptor blockade prevents synaptotoxicity and memory dysfunction caused by beta-amyloid peptides via p38 mitogen-activated protein kinase pathway. *J Neurosci* 2009b; 29: 14741–51.
- Canas PM, Porciúncula LO, Simões AP, Augusto E, Silva HB, Machado NJ, et al. Neuronal adenosine A<sub>2A</sub> receptors are critical mediators of neurodegeneration triggered by convulsions. *eNeuro* 2018; 5: ENEURO.0385-18.2018.
- Gonçalves FQ, Lopes JP, Silva HB, Lemos C, Silva AC, Gonçalves N, et al. Synaptic and memory dysfunction in a β-amyloid model of early Alzheimer's disease depends on increased formation of ATP-derived extracellular adenosine. *Neurobiol Dis* 2019; 132: 104570. doi: 10.1016/j.nbd.2019.104570.
- Chatterjee S, Cassel R, Schneider-Anthony A, Merienne K, Cosquer B, Tzeplaff L, et al. Reinstating plasticity and memory in a tauopathy mouse model with an acetyltransferase activator. *EMBO Mol Med* 2018; 10: pii: e8587. doi: 10.15252/emmm.201708587.
- Costenla AR, Diógenes MJ, Canas PM, Rodrigues RJ, Nogueira C, Maroco J, et al. Enhanced role of adenosine A<sub>2A</sub> receptors in the modulation of LTP in the rat hippocampus upon ageing. *Eur J Neurosci* 2011; 34: 12–21.
- Cunha RA. How does adenosine control neuronal dysfunction and neurodegeneration? *J Neurochem* 2016; 139: 1019–55.
- Dejanovic B, Huntley MA, De Mazière A, Meilandt WJ, Wu T, Srinivasan K, et al. Changes in the synaptic proteome in tauopathy and rescue of tau-induced synapse loss by C1q antibodies. *Neuron* 2018; 100: 1322–36.e7.
- Duyckaerts C, Bennefib M, Grignon Y, Uchihara T, He Y, Piette F, et al. Modeling the relation between neurofibrillary tangles and intellectual status. *Neurobiol Aging* 1997; 18: 267–73.
- Duyckaerts C, Braak H, Brion J-P, Buée L, Del Tredici K, Goedert M, et al. PART is part of Alzheimer disease. *Acta Neuropathol* 2015; 129: 749–56.
- Faivre E, Coelho JE, Zornbach K, Malik E, Baqi Y, Schneider M, et al. Beneficial effect of a selective adenosine A<sub>2A</sub> receptor antagonist in the APP<sup>swe</sup>/PS1<sup>dE9</sup> mouse model of Alzheimer's Disease. *Front Mol Neurosci* 2018; 11: 235.
- Fonseca MI, Chu S-H, Hernandez MX, Fang MJ, Modarresi L, Selvan P, et al. Cell-specific deletion of C1qa identifies microglia as the dominant source of C1q in mouse brain. *J Neuroinflammation* 2017; 14: 48.
- Fonseca MI, Kawas CH, Troncoso JC, Tenner AJ. Neuronal localization of C1q in preclinical Alzheimer's disease. *Neurobiol Dis* 2004; 15: 40–6.
- Forrest SL, Kril JJ, Stevens CH, Kwok JB, Hallupp M, Kim WS, et al. Retiring the term FTDP-17 as MAPT mutations are genetic forms of sporadic frontotemporal tauopathies. *Brain* 2018; 141: 521–34.
- Gonçalves FQ, Lopes JP, Silva HB, Lemos C, Silva AC, Gonçalves N, et al. Synaptic and memory dysfunction in a β-amyloid model of early Alzheimer's disease depends on increased formation of ATP-derived extracellular adenosine. *Neurobiol Dis* 2019; 132: 104570. doi: 10.1016/j.nbd.2019.104570.
- Grober E, Dickson D, Sliwinski MJ, Buschke H, Katz M, Crystal H, et al. Memory and mental status correlates of modified Braak staging. *Neurobiol Aging* 1999; 20: 573–9.
- Guan Z, Kuhn JA, Wang X, Colquitt B, Solorzano C, Vaman S, et al. Injured sensory neuron-derived CSF1 induces microglial proliferation and DAP12-dependent pain. *Nat Neurosci* 2016; 19: 94–101.
- Han HJ, Allen CC, Buchovecky CM, Yetman MJ, Born HA, Marin MA, et al. Strain background influences neurotoxicity and behavioral abnormalities in mice expressing the tetracycline transactivator. *J Neurosci* 2012; 32: 10574–86.
- Hamdane M, Buée L. The complex p25/Cdk5 kinase in neurofibrillary degeneration and neuronal death: the missing link to cell cycle. *Biotechnol J* 2007; 2: 967–77.
- Holtman IR, Raj DD, Miller JA, Schaafsma W, Yin Z, Brouwer N, et al. Induction of a common microglia gene expression signature by aging and neurodegenerative conditions: a co-expression meta-analysis. *Acta Neuropathol Commun* 2015; 3: 31.
- Hong S, Beja-Glasser VF, Nfonoyim BM, Frouin A, Li S, Ramakrishnan S, et al. Complement and microglia mediate early synapse loss in Alzheimer mouse models. *Science* 2016; 352: 712–6.
- Huang DW, Sherman BT, Lempicki RA. Systematic and integrative analysis of large gene lists using DAVID bioinformatics resources. *Nat Protoc* 2009; 4: 44–57.
- Huin V, Deramecourt V, Caparros-Lefebvre D, Maurage C-A, Duyckaerts C, Kovari E, et al. The MAPT gene is differentially methylated in the progressive supranuclear palsy brain. *Mov Disord* 2016; 31: 1883–90.
- Hutton M, Lendon CL, Rizzu P, Baker M, Froelich S, Houlden H, et al. Association of missense and 5'-splice-site mutations in tau with the inherited dementia FTDP-17. *Nature* 1998; 393: 702–5.
- Josephs KA, Murray ME, Tosakulwong N, Whitwell JL, Knopman DS, Machulda MM, et al. Tau aggregation influences cognition and hippocampal atrophy in the absence of beta-amyloid: a clinico-imaging-pathological study of primary age-related tauopathy (PART). *Acta Neuropathol* 2017; 133: 705–15.
- Jucker M, Walker LC. Self-propagation of pathogenic protein aggregates in neurodegenerative diseases. *Nature* 2013; 501: 45–51.
- Kaster MP, Machado NJ, Silva HB, Nunes A, Ardais AP, Santana M, et al. Caffeine acts through neuronal adenosine A<sub>2A</sub> receptors to prevent mood and memory dysfunction triggered by chronic stress. *Proc Natl Acad Sci USA* 2015; 112: 7833–8.
- Kelly PT, Shields S, Conway K, Yip R, Burgin K. Developmental changes in calmodulin-kinase II activity at brain synaptic junctions: alterations in holoenzyme composition. *J Neurochem* 1987; 49: 1927–40.
- Keren-Shaul H, Spinrad A, Weiner A, Matcovitch-Natan O, Dvir-Szternfeld R, Ulland TK, et al. A unique microglia type associated with restricting development of Alzheimer's disease. *Cell* 2017; 169: 1276–90.e17.
- Kozak M. An analysis of 5'-noncoding sequences from 699 vertebrate messenger RNAs. *Nucleic Acids Res* 1987; 15: 8125–48.
- Langmead B, Schatz MC, Lin J, Pop M, Salzberg SL. Searching for SNPs with cloud computing. *Genome Biol* 2009; 10: R134.
- Laurent C, Burnouf S, Ferry B, Batalha VL, Coelho JE, Baqi Y, et al. A<sub>2A</sub> adenosine receptor deletion is protective in a mouse model of tauopathy. *Mol Psychiatry* 2016; 21: 97–107.
- Laurent C, Dorothée G, Hunot S, Martin E, Monnet Y, Duchamp M, et al. Hippocampal T cell infiltration promotes neuroinflammation and cognitive decline in a mouse model of tauopathy. *Brain* 2017; 140: 184–200.

- Leboucher A, Laurent C, Fernandez-Gomez F-J, Burnouf S, Troquier L, Eddarkaoui S, et al. Detrimental effects of diet-induced obesity on pathology are independent of insulin resistance in transgenic mice. *Diabetes* 2013; 62: 1681–8.
- Lebouvier T, Pasquier F, Buée L. Update on tauopathies. *Curr Opin Neurol* 2017; 30: 589–98.
- Lee C-C, Chang C-P, Lin C-J, Lai H-L, Kao Y-H, Cheng S-J, et al. Adenosine augmentation evoked by an ENT1 inhibitor improves memory impairment and neuronal plasticity in the APP/PS1 mouse model of Alzheimer's disease. *Mol Neurobiol* 2018; 55: 8936–52.
- Li P, Rial D, Canas PM, Yoo J-H, Li W, Zhou X, et al. Optogenetic activation of intracellular adenosine A2A receptor signaling in the hippocampus is sufficient to trigger CREB phosphorylation and impair memory. *Mol Psychiatry* 2015; 20: 1339–49.
- Lopes LV, Cunha RA, Ribeiro JA. Increase in the number, G protein coupling, and efficiency of facilitatory adenosine A2A receptors in the limbic cortex, but not striatum, of aged rats. *J Neurochem* 1999; 73: 1733–8.
- Lopes S, Vaz-Silva J, Pinto V, Dalla C, Kokras N, Bedenk B, et al. Tau protein is essential for stress-induced brain pathology. *Proc Natl Acad Sci* 2016; 113: E3755–63.
- Love MI, Huber W, Anders S. Moderated estimation of fold change and dispersion for RNA-seq data with DESeq2. *Genome Biol* 2014; 15: 550.
- Luo J, Elwood F, Britschgi M, Villeda S, Zhang H, Ding Z, et al. Colony-stimulating factor 1 receptor (CSF1R) signaling in injured neurons facilitates protection and survival. *J Exp Med* 2013; 210: 157–72.
- Machado RA, Benjumea-Cuartas V, Zapata Berruecos JF, Agudelo-Flóres PM, Salazar-Peláez LM. Reelin, tau phosphorylation and psychiatric complications in patients with hippocampal sclerosis and structural abnormalities in temporal lobe epilepsy. *Epilepsy Behav* 2019; 96: 192–9.
- Machado NJ, Simões AP, Silva HB, Ardais AP, Kaster MP, Garção P, et al. Caffeine reverts memory but not mood impairment in a depression-prone mouse strain with up-regulated adenosine A2A receptor in hippocampal glutamate synapses. *Mol Neurobiol* 2017; 54: 1552–63.
- Mackenzie IRA, Neumann M. Molecular neuropathology of fronto-temporal dementia: insights into disease mechanisms from postmortem studies. *J Neurochem* 2016; 138: 54–70.
- Mathys H, Adakkan C, Gao F, Young JZ, Manet E, Hemberg M, et al. Temporal tracking of microglia activation in neurodegeneration at single-cell resolution. *Cell Rep* 2017; 21: 366–80.
- Matos M, Augusto E, Machado NJ, dos Santos-Rodrigues A, Cunha RA, Agostinho P. Astrocytic adenosine A2A receptors control the amyloid- $\beta$  peptide-induced decrease of glutamate uptake. *J Alzheimers Dis* 2012; 31: 555–67.
- Orr AG, Hsiao EC, Wang MM, Ho K, Kim DH, Wang X, et al. Astrocytic adenosine receptor A2A and Gs-coupled signaling regulate memory. *Nat Neurosci* 2015; 18: 423–34.
- Orr AG, Lo I, Schumacher H, Ho K, Gill M, Guo W, et al. Istradefylline reduces memory deficits in aging mice with amyloid pathology. *Neurobiol Dis* 2018; 110: 29–36.
- Paiva I, Carvalho K, Santos P, Cellai L, Angeliki Maria et al. A2AR-induced transcriptional deregulation in astrocytes: an in vitro study. *Glia* 2019. doi: 10.1002/glia.23688.
- Plescher M, Seifert G, Hansen JN, Bedner P, Steinhäuser C, Halle A. Plaque-dependent morphological and electrophysiological heterogeneity of microglia in an Alzheimer's disease mouse model. *Glia* 2018; 66: 1464–80.
- Rebola N, Sebastião AM, de Mendonça A, Oliveira CR, Ribeiro JA, Cunha RA. Enhanced adenosine A2A receptor facilitation of synaptic transmission in the hippocampus of aged rats. *J Neurophysiol* 2003; 90: 1295–303.
- Rodrigues RJ, Marques JM, Cunha RA. Purinergic signalling and brain development. *Semin Cell Dev Biol* 2018, pii: S1084-9521. doi: 10.1016/j.semcdb.2018.12.001.
- Schafer DP, Lehrman EK, Kautzman AG, Koyama R, Mardinly AR, Yamasaki R, et al. Microglia sculpt postnatal neural circuits in an activity and complement-dependent manner. *Neuron* 2012; 74: 691–705.
- Schindowski K, Bretteville A, Leroy K, Bégard S, Brion J-P, Hamdane M, et al. Alzheimer's disease-like tau neuropathology leads to memory deficits and loss of functional synapses in a novel mutated tau transgenic mouse without any motor deficits. *Am J Pathol* 2006; 169: 599–616.
- Scholz WK, Baitinger C, Schulman H, Kelly PT. Developmental changes in Ca<sup>2+</sup>/calmodulin-dependent protein kinase II in cultures of hippocampal pyramidal neurons and astrocytes. *J Neurosci* 1988; 8: 1039–51.
- Sergeant N, Bretteville A, Hamdane M, Caillet-Boudin M-L, Grognet P, Bombois S, et al. Biochemistry of Tau in Alzheimer's disease and related neurological disorders. *Expert Rev Proteomics* 2008; 5: 207–24.
- Silva AC, Lemos C, Gonçalves FQ, Pliássova AV, Machado NJ, Silva HB, et al. Blockade of adenosine A2A receptors recovers early deficits of memory and plasticity in the triple transgenic mouse model of Alzheimer's disease. *Neurobiol Dis* 2018; 117: 72–81.
- Spires-Jones TL, Hyman BT. The intersection of amyloid beta and tau at synapses in Alzheimer's disease. *Neuron* 2014; 82: 756–71.
- Srinivasan K, Friedman BA, Larson JL, Lauffer BE, Goldstein LD, Appling LL, et al. Untangling the brain's neuroinflammatory and neurodegenerative transcriptional responses. *Nat Commun* 2016; 7: 11295.
- Stephan AH, Madison DV, Mateos JM, Fraser DA, Lovelett EA, Coutellier L, et al. A dramatic increase of C1q protein in the CNS during normal aging. *J Neurosci* 2013; 33: 13460–74.
- Szklarczyk D, Morris JH, Cook H, Kuhn M, Wyder S, Simonovic M, et al. The STRING database in 2017: quality-controlled protein-protein association networks, made broadly accessible. *Nucleic Acids Res* 2017; 45: D362–8.
- Temido-Ferreira M, Ferreira DG, Batalha VL, Marques-Morgado I, Coelho JE, Pereira P, et al. Age-related shift in LTD is dependent on neuronal adenosine A2A receptors interplay with mGluR5 and NMDA receptors. *Mol Psychiatry* 2018, doi: 10.1038/s41380-018-0110-9.
- Trapnell C, Pachter L, Salzberg SL. TopHat: discovering splice junctions with RNA-Seq. *Bioinformatics* 2009; 25: 1105–11.
- Van der Jeugd A, Ahmed T, Burnouf S, Belarbi K, Hamdane M, Grosjean M-E, et al. Hippocampal tauopathy in tau transgenic mice coincides with impaired hippocampus-dependent learning and memory, and attenuated late-phase long-term depression of synaptic transmission. *Neurobiol Learn Mem* 2011; 95: 296–304.
- Van der Jeugd A, Vermaercke B, Derisbourg M, Lo AC, Hamdane M, Blum D, et al. Progressive age-related cognitive decline in tau mice. *J Alzheimers Dis* 2013; 37: 777–88.
- Vasek MJ, Garber C, Dorsey D, Durrant DM, Bollman B, Soung A et al. A complement-microglial axis drives synapse loss during virus-induced memory impairment. *Nature* 2016; 534: 538–43.
- Viana da Silva S, Haberl MG, Zhang P, Bethge P, Lemos C, Gonçalves N, et al. Early synaptic deficits in the APP/PS1 mouse model of Alzheimer's disease involve neuronal adenosine A2A receptors. *Nat Commun* 2016; 7: 11915.
- Wohleb ES. Neuron-microglia interactions in mental health disorders: “For Better, and For Worse.” *Front Immunol* 2016; 7: 544.
- Wohleb ES, Terwilliger R, Duman CH, Duman RS. Stress-induced neuronal CSF1 provokes microglia-mediated neuronal remodeling and depressive-like behavior. *Biol Psychiatry* 2018; 83: 38–49.
- Zhang Y, Chen K, Sloan SA, Bennett ML, Scholze AR, O'Keefe S, et al. An RNA-sequencing transcriptome and splicing database of glia, neurons, and vascular cells of the cerebral cortex. *J Neurosci* 2014; 34: 11929–47.